

RESEARCH

Open Access



Bioinformatics based exploration of the anti-NAFLD mechanism of Wang's empirical formula via TLR4/NF- κ B/COX2 pathway

Suhong Chen^{1,3,4†}, Chuanjie Zhou^{1,3†}, Jiahui Huang^{1,3†}, Yunlong Qiao^{1,3†}, Ning Wang^{1,3}, Yuzhen Huang^{1,3}, Bo Li^{1,3}, Wanfeng Xu^{1,3}, Xinglishang He^{1,3}, Kungen Wang^{2,5*}, Yihui Zhi^{2,5*}, Guiyuan Lv^{4*} and Shuhua Shen^{2,5*}

Abstract

Background Nonalcoholic fatty liver disease (NAFLD) has developed as a leading public wellness challenge as a result of changes in dietary patterns. Unfortunately, there is still a lack of effective pharmacotherapy methods for NAFLD. Wang's empirical formula (WSF) has demonstrated considerable clinical efficacy in treating metabolic disorders for years. Nevertheless, the protective effect of WSF against NAFLD and its underlying mechanism remains poorly understood.

Methods The NAFLD model was established using a 17-week high-sucrose and high-fat (HSHF) diet with 32 ICR mice. In assessing the therapeutic efficacy of WSF on NAFLD, we detected changes in body weight, viscera weight, biomarkers of glycolipid metabolism in serum and liver, transaminase levels and histopathology of liver with H&E and Oil Red O staining after oral administration. The chemical components in WSF were extensively identified and gathered utilizing the HPLC-Q-TOF/MS system, database mining from HMDB, MassBank, and TCMSP databases, alongside literature searches from CNKI, Wanfang and VIP databases. The forecast of network pharmacology approach was then utilized to investigate the probable mechanisms by which WSF improves NAFLD based on the performance of prospective target identification and pathway enrichment analysis. Besides, molecular docking was also conducted for the verification of combination activities between active components of WSF and core proteins related to NAFLD. In final, validation experiments of obtained pathways were conducted through ELISA, immunohistochemistry (IHC), and western blot (WB) analysis.

Results Pharmacodynamic outcomes indicated that WSF intervention effectively mitigated obesity, fat accumulation in organs, lipid metabolism disorders, abnormal transaminase levels and liver pathology injury in NAFLD mice

[†]Suhong Chen, Chuanjie Zhou, Jiahui Huang and Yunlong Qiao shared co-first authorship.

*Correspondence:

Kungen Wang
wkg1220@163.com
Yihui Zhi
medcat4@163.com
Guiyuan Lv
zjtcmlgy@163.com
Shuhua Shen
linda0358@163.com

Full list of author information is available at the end of the article



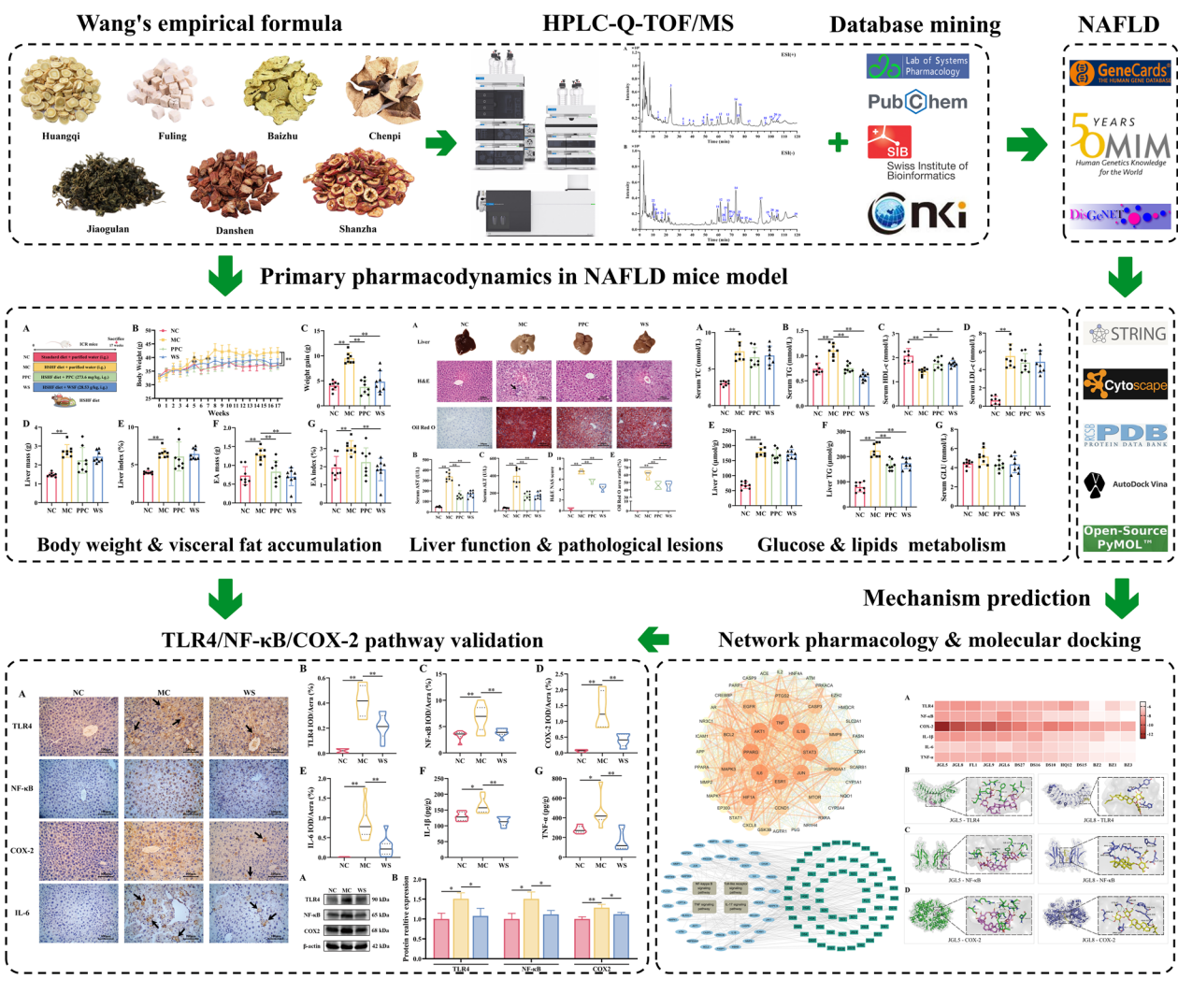
© The Author(s) 2024. **Open Access** This article is licensed under a Creative Commons Attribution 4.0 International License, which permits use, sharing, adaptation, distribution and reproduction in any medium or format, as long as you give appropriate credit to the original author(s) and the source, provide a link to the Creative Commons licence, and indicate if changes were made. The images or other third party material in this article are included in the article's Creative Commons licence, unless indicated otherwise in a credit line to the material. If material is not included in the article's Creative Commons licence and your intended use is not permitted by statutory regulation or exceeds the permitted use, you will need to obtain permission directly from the copyright holder. To view a copy of this licence, visit <http://creativecommons.org/licenses/by/4.0/>.

($P < 0.05, 0.01$). A total of 72 existent ingredients of WSF were acquired by HPLC-Q-TOF/MS and database, and 254 common targets (11.6% in total targets) of NAFLD and WSF were identified. Network pharmacology revealed that WSF presses NAFLD via modulating TNF, IL6, AKT1, IL1B, PTGS2 (COX2), and other targets, and the probable pathways were primarily inflammatory signaling pathways, as confirmed by molecular docking. Molecular biology experiments further conformed that WSF could decrease levels of inflammatory factors like IL-1 β , IL-6 and TNF- α ($P < 0.01$) and expression of TLR4, NF- κ B and COX-2 ($P < 0.05, 0.01$) in the liver.

Conclusion WSF treatment effectively protects against lipid metabolism disorders and liver inflammation injury in HSHF diet-induced NAFLD mice, and its molecular mechanism might be via suppressing the TLR4/NF- κ B/COX-2 inflammatory pathway to reduce the release of inflammatory cytokines in the liver.

Keywords Nonalcoholic fatty liver disease, Wang's empirical formula, Liver inflammation, HPLC-Q-TOF/MS, Bioinformatics, Network pharmacology

Graphical abstract



Introduction

Due to alterations in dietary patterns, nonalcoholic fatty liver disease (NAFLD) caused by overnutrition and metabolic disorders has become a common chronic liver disease globally (Younossi et al. 2018). NAFLD is appraised to afflict approximately 25% of the world population with a gradual upward trend (Younossi et al. 2019). The total adult NAFLD prevalence have been reported as high as 29.81% in China, and it is predicated that there will be 314.58 million NAFLD patients in 2030 if without effective control (Li et al. 2019a, b; Zhou et al. 2019). NAFLD is typically divided into two subtypes: nonalcoholic fatty liver (NAFL, with mild symptoms) and nonalcoholic steatohepatitis (NASH, with steatosis of hepatocytes, aggravated inflammatory reaction, and irreversible hepatocyte damage like ballooning transformation) (Loomba et al. 2021). Progression from NAFLD can lead to liver fibrosis, cirrhosis and even liver cancer at a later stage, causing a tremendous burden on human health. Therefore, a penetrative study on the pathophysiology and management of NAFLD has important practical significance.

At present, there is still a lack of effective pharmacotherapy methods for NAFLD (Tilg et al. 2023). Instead, it is recommended to change unhealthy lifestyle like improving dietary structure and lifestyle modifications such as exercise to mitigate the progression of NAFLD firstly (Houttu et al. 2021; Xiong et al. 2021). The mainstay of drug treatments for NAFLD lies in the inhibition of lipid accumulation and protection of liver damage (include hepatic fibrosis). However, some drugs suffer from incomplete therapeutic efficacy or adverse reactions during clinical use, for instance statins might cause elevations of hepatic aminotransferase levels, high risks of new-onset diabetes, myopathy and even myalgias or rhabdomyolysis (Dong et al. 2014). Therefore, search for safer and more effective drugs for NAFLD treatment is imperative.

Traditional Chinese medicine (TCM) is recognized for its unique action modes of multi-target and multi-channel, and there is plenty of testimony that TCM plays a significant role in NAFLD prevention and treatment (Shi et al. 2020; Chen et al. 2021a, b). Wang's empirical formula (WSF) was a clinical empirical formula developed for the remedy of metabolic diseases by Prof. Wang Kun-Gen, the first national famous doctor of TCM and national academic leader of "spleen and stomach disease of TCM" (Shen et al. 2018). WSF is derived from the classic traditional formula Er-Chen Decoction, and is composed of *Gynostemmae Herba* (Jiaogulan), *Astragali Radix* (Huangqi), *Crataegi Fructus* (Shanzha), *Salviae Miltiorrhizae Radix et Rhizoma* (Danshen), and *Poria* (Fuling), etc. Meanwhile, WSF has the impact of "invigorating the spleen and benefiting the stomach, clearing heat

and promoting diuresis", which is congruent with the TCM's therapy theory for NAFLD. Despite WSF demonstrates a certain therapeutic efficacy in treating NAFLD, the underlying mechanism of its action remains elusive.

At present, the pathogenesis and development process of NAFLD are quite complex and without comprehensive explanation. The "two-hit" hypothesis initially proposed in 1998 is considered as the classic pathogenesis of NAFLD (Day and James 1998). The first hit mainly included factors like the sedentary lifestyle and poor nutritional habits, resulting in excessive intrahepatic fat accumulation (triglyceride in main) and insulin resistance. The second hit was characterized by the overproduction of lipid-induced reactive oxidative metabolites, which in turn led to the cytokines-mediated inflammation, hepatic cell apoptosis, necrosis, fibrosis and cirrhosis in final (Berardo et al. 2020). With the deepening of research, the "two-hit" hypothesis gradually evolved into the "multiple-hit" hypothesis for a precise explanation of the etiology and pathogenesis behind NAFLD. The core idea of this theory suggested that multiple hits like nutritional factors, insulin resistance, lipotoxicity, inflammatory cascades, gut microbiota could play a role at the same time, and each factor contributed to the further progression of the disease (Buzzetti et al. 2016; Wu et al. 2022).

The TLR4/NF- κ B-dependent release of inflammatory cytokines (such as TNF- α , IL-6 and IL-1 β) is regarded as one of important mechanisms of NAFLD (Bessone et al. 2019). Existing studies have proved that inhibiting this pathway can improve lipid metabolism disorders in NAFLD mice and alleviate the inflammatory state of the liver (Chen et al. 2024; Deng et al. 2024), proving that inhibition of the TLR4/NF- κ B signaling pathway is a potential therapeutic approach for NAFLD. COX-2 is highly expressed in inflamed tissues and it can produce inflammatory cytokines prostaglandin E2 (PGE2) from arachidonic acid (Yagami et al. 2016). Moreover, TLR4/NF- κ B signaling also regulates the activation of the COX2/PGE2 axis in liver fibrosis, indicating that COX2 also plays a role in the inflammatory regulation of liver diseases (Chen et al. 2021a, b; Yang et al. 2020).

Network pharmacology employs high-throughput omics data analysis, network database retrieval and computer simulation to uncover the network relationship of herb-gene-target-disease interaction. Through delineating these intricate networks, it can predict the evaluate medicine efficacy and exact mechanisms of medicine action in disease treatment of TCM. (Shi et al. 2023; Li et al. 2022; Zheng et al. 2024). Based on this theoretical method, Wu et al. verified the mechanism of Qutan Huoxue decoction on NASH via inhibiting the SOCS1/TLR4/NF- κ B inflammatory pathway with network

pharmacology and *in vitro* experiments (Wu et al. 2023). Widespread application of HPLC-Q-TOF/MS has been employed in the structural determination of unknown chemicals in complicated mixtures via retention time, molecular mass and fragment information, which is effective in identifying probable active substances in TCM (Zhou et al. 2021; Jin et al. 2023). In addition, the integration of HPLC-Q-TOF/MS with network pharmacology has also greatly promoted the credibility of research conclusions (Zhi et al. 2023; Wang et al. 2022).

Molecular docking represents a pivotal structure-guided technique that facilitates the meticulous examination of the intricate binding interactions between protein targets and potential small-molecule ligands (Kaur et al. 2019). It was integrated synergistically within pharmacological investigations of TCM alongside network pharmacology, wherein their computationally derived predictions undergo experimental validation as a means to substantiate their findings (Liu et al. 2022; Bai et al. 2023; Jiao et al. 2021). The comprehensive advantage of network pharmacology combined with molecular docking is that it provides concepts for the investigation of complex TCM, which is progressively being used in the study of NAFLD pathogenesis and treatment (Ren et al. 2022).

Therefore, we firstly detected the therapeutic effects of WSF against NAFLD by evaluating the biochemical indices and histopathology in a high-sucrose and high-fat (HSHF) diet mice. Moreover, HPLC-Q-TOF/MS, bioinformatics in conjugation with molecular docking were applied to plumb the probable mechanism of WSF for the therapy of NAFLD in this research. Finally, we further validated the predicted pathway by immunohistochemistry, ELISA and western blot using liver tissue from the efficacy experiment *in vivo*. This study would offer persuasive evidence for the clinical promotion of WSF later.

Materials and methods

Chemical and biological reagents

Polyene Phosphatidylcholine (Essentiale, PPC) capsule was gained from Sanofi–Aventis Pharmaceutical Co., Ltd. (Beijing, China). Total cholesterol (TC), triglyceride (TG), high density lipoprotein cholesterol (HDL-c), glucose (GLU), aspartate transaminase (AST), alanine transferase (ALT) assay kits were obtained from Ningbo Medical System Biotechnology Co., Ltd. (Ningbo, China). Hematoxylin–Eosin (H&E) reagent was acquired from Shanghai Yuanye Biotechnology Co., Ltd. (Shanghai, China). Oil red O reagent was purchased from BBI Life Science Corporation (Shanghai, China). TC and TG assay kits for liver were both attained from Nanjing Jiancheng Bioengineering Institute (Nanjing, China). The ELISA kits of IL-1 β and TNF- α were derived from Jiangsu

Meimian Industrial Co., Ltd. (Yancheng, China). Instant immunohistochemistry kits were gained from Wuhan Boster Biological Technology Co., Ltd. (Wuhan, China). The DAB staining kit, BCA assay kit, RIPA buffer, and protein free rapid blocking buffer were got from Beyotime Biotechnology Reagent Co., Ltd. (Shanghai, China). The antibodies of COX2, IL-6 and secondary antibodies were purchased from Proteintech Group Inc. (Wuhan, China). The antibodies for TLR4, NF- κ B and β -actin were acquired from Beijing Biosynthesis Biotechnology Co., Ltd. (Beijing, China), Hangzhou DiagBio Biotechnology Co., Ltd. (Hangzhou, China), and Wuhan Servicebio Technology Co., Ltd. (Wuhan, China), respectively. The enhanced chemiluminescent assay kit was attained from Nature Biosciences Ltd. (Hangzhou, China). The catalog numbers of utilized reagents are included in supplementary file.

Drug preparation

WSF was prepared by the Traditional Chinese Medicine Health Products Institute of Zhejiang University of Technology, and was then condensed to concentration of 2.853 g/mL in crude herb amounts. It was then refrigerated in 4 °C for later use.

Animal experiment

ICR mice (male, n=32) were purchased from Laboratory Animal Center of Zhejiang Academy of Medical Sciences (SYXK(Zhe)2019–002, Hangzhou, China). All the animals were reared in standardized environmental conditions characterized by a 12-h light–dark photoperiod with unrestricted access to water and food. The animal procedures were meticulously conducted in strict adherence to the Zhejiang University of Technology's Guidelines for the Care and Use of Laboratory Animals.

Our group previously established that the ideal concentration of WSF for treating rats with glucose and lipid metabolic disorders is 14.26 g/kg (detailed data is in supplementary file). And for this study, the dosage for NAFLD mice was determined to be 28.53 g/kg based on the specific surface area method for animal dose conversion.

Considering the optimal dosage was determined and the principle of reduction in animal experiments, we used a single dosage in this study. After adaptive feeding for 1 week, a total of 32 ICR mice were randomly assigned into four groups according to their body weight with the random number method: the normal group (NC), the model group (MC), PPC administration group (PPC) and WSF administration group (WS), each consisting of 8 mice. The NC mice was fed with standard diet, while mice in the MC, PPC and WS group were all received a high-sucrose and high-fat

(HSHF) diet over a period of 17 weeks. The PPC and WS mice were daily administered PPC or WSF at a dose of 273.6 mg/kg or 28.53 g/kg (i.g.) adjusted to the volume of 1 ml/100 g in accordance with the body weight, respectively. The HSHF diet, consisting of 10% lard, 10% egg yolk powder, 5% sucrose, 2% cholesterol, 0.5% sodium cholate was derived from Trophic Animal Feed High-Tech Co.,Ltd. (Nantong, China).

Upon conclusion of the experiment, mice were subjected to an overnight fasting before blood was drawn from the ocular venous plexus. Obtained blood samples were centrifuged for 10 min twice at 3600 rpm to attain serum for biochemical analysis. The mice were subsequently anesthetized (isoflurane inhalation) with removing their liver as quickly as possible. Part of liver was put in 4% paraformaldehyde tissue fixation solution for hepatic pathology and immunohistochemistry analysis, part of liver was put in ethanol absolute for liver homogenate and remaining parts were preserved at -80°C .

Moreover, we conducted a separate 28-day oral toxicity experiment (detailed data are provided in the supplementary file), which demonstrated that administration at 12 times the human clinical dose did not exhibit significant toxic effects on the liver or glucose and lipid metabolism in normal mice.

Histological staining

The Hematoxylin–eosin (H&E) and Oil Red O staining procedures were conducted consistent with the methods detailed in prior literature (Lei et al. 2019). H&E staining were undergone on 4 μm paraffin-embedded tissue slices and liver pathology scores for NAFLD were decided in line with NAFLD activity score (NAS) nominated by American Association for the Study of Liver Diseases as Table 1 described (Kleiner et al. 2005). The specific procedures of tissue dehydration and the H&E staining are described in the supplementary file.

Oil Red O staining serves as a reliable method for both the identification of lipid accumulation and the semi-quantitative assessment of hepatic steatosis. In brief, liver tissue specimens were first dehydrated in a 30% sucrose solution prior to being embedded in OCT as well as sliced into 10 μm -thick frozen sections. The 0.5% Oil Red O solution was subsequently stained on the obtained cryosections, followed by hematoxylin counterstaining on the nuclei. All H&E and Oil Red O stains were captured under the biological microscope (BX43, Olympus, Japan) and subjected to semi-analysis using the Image J software (version 1.54f). The code used for Oil Red O analysis are included in supplementary file.

Table 1 Scoring standard of NAFLD activity

NAS (0–8 points)	
1. Steatosis (0–3 points)	
0	< 5%
1	5–33%
2	33–66%
3	> 66%
2. Lobular inflammation (0–3 points)	
0	No foci
1	< 2 foci in 200 \times vision
2	2–4 foci in 200 \times vision
3	> 4 foci in 200 \times vision
3. Ballooning (0–2 points)	
0	None
1	Few
2	Many or prominent ballooning

Measurement of biomarkers in serum and liver

Serum blood glucose (GLU), transaminase (AST and ALT), and lipid levels (TC, TG, and HDL-c) were determined with the respective assay reagents on the automated biochemical analyzer (HITACHI-7020, Japan). The level of serum LDL-c was further calculated by Friedwald formula (Molavi et al. 2020).

Friedwald formula : $\text{LDL} - \text{c} = \text{TC} - \text{HDL} - \text{c} - \text{TG}/5$

To measure the concentrations of TC and TG in the liver, liver organs (circa 100 mg) were put into ethanol absolute (9 times in volume), homogenized for a 10% (w/v) homogenate solution and centrifuged at 2500 rpm for 10 min twice later for the acquisition of supernatant. After mixing the 2.5 μL tissue extract solution with 250 μL working solution and allowing it to stand for 10 min at 37°C , we measured the absorbance at a wavelength of 500 nm (TC) or 510 nm (TG), respectively. The specific concentrations of TC and TG were calculated through the standard curve.

Qualitative identification of components in WSF

Sample preparation

The WSF powder was obtained using the vacuum freeze dryer (-55°C , 20 Pa). Then, 3.0 g WSF powder was extracted ultrasonically (40 kHz, 300 W, likewise below) for 60 min with 30 mL methanol (chromatographic purity, likewise below) and the resultant solution was evaporated in an 85°C water bath until dryness. Another 3 mL methanol was used to redissolve the residue with ultrasound for 30 min. Finally, 1.0 mL supernatant fluid underwent filtration via a 0.22 μm organic phase filter

membrane with the syringe and relocated in a sampling vial for qualitative analysis.

HPLC-Q-TOF/MS conditions

The HPLC-Q-TOF/MS system was composed of a 1290 Infinity II liquid chromatography and a 6545XT AdvanceBio Quadruple Time-of-Flight mass spectrometry (Agilent Technologies, USA).

The chromatographic conditions were as follows: (1) Column: Welch Ultimate LP-C18 (4.6×250 mm, 5 μm); (2) Injection volume: 10 μL; (3) Column temperature: 30°C; (4) Flow rate: 1 mL/min; (5) Mobile phase A: water (comprising 0.1% formic acid, analytical purity), B: acetonitrile (chromatographic purity) with the changeable gradient of 0 min, 5% B; 10 min, 10% B; 40 min, 13% B; 55 min, 16% B; 65 min, 20% B; 90 min, 21% B; 100 min, 26% B; 120 min, 28% B.

The operating conditions of mass spectrometry were set as follows: (1) Ion source: Agilent jet stream electrospray ionization source (AJS-ESI); (2) Gas flow rate: 8 L/min; (3) Gas temperature: 300 °C; (4) Sheath gas temperature: 350 °C; (5) Nebulizer gas pressure: 35 psi; (6) Sheath gas flow rate: 11 L/min; (7) Capillary voltage: 3100 V; (8) Fragmentor voltage: 175 V; (9) Nozzle Voltage: 1000 V. Scanning with a range of *m/z* 50–3200 was utilized for sample mass spectrometry signal acquisition in positive and negative ion modes, respectively. All of the collected data were processed utilizing the Agilent MassHunter workstation software (version B.08.00).

Bioinformatics analysis

Prediction of prospective WSF targets associated to NAFLD

The components of herbs in WSF were also collected with the TCMSP database (<https://old.tcmssp-e.com/tcmssp.php>, version 2.3), while the bioactive ingredients of Shanzha were identified by a supplemented literature search due to the lack in the TCMSP database (Cheng et al. 2023). The chemical components obtained from HPLC-Q-TOF/MS and database mining were sifted with a criterion of oral bioavailability ($OB \geq 30\%$) and drug-like properties ($DL \geq 0.18$) as well as further screened through the Swiss ADME (<http://www.swissadme.ch/index.php>) platform with a score of “High” for gastrointestinal absorption and at least two “Yes” for drug like properties. The filtered ingredients were later transmitted to the Swiss Target Prediction platform (<http://www.swisstargetprediction.ch>) for protein target search with their canonical SMILES attained from PubChem database (<https://pubchem.ncbi.nlm.nih.gov>). The targets with a credibility value of 0 were deleted.

GeneCards (<https://www.genecards.org>, version 5.22.0 Build 1354), DisGENET (<https://www.disgenet.org>, version 24.3) and OMIM database (<https://www.omim.org>)

were applied to obtain the NAFLD-relevant protein targets, and the keywords were set as “non-alcoholic fatty liver disease”. Targets from GeneCards database that not exceeding the median relevance scores were eliminated, and duplicate entries were consolidated to derive the set of NAFLD-related targets. Finally, the herbs-active components-targets network was constructed and visualized via Cytoscape 3.7.1 software after standardization of names with Uniprot database (<https://www.uniprot.org>, release 2024_05).

“Network analyzer” function in Cytoscape 3.7.1 was conducted to evaluate the overall situation of the network with topological parameters encompassing degree, average shortest path length (ASPL), betweenness centrality (BNC) and closeness centrality (CNC).

Coincident targets identification and protein–protein interaction (PPI) network analysis

The intersectional analysis of Venny 2.1.0 (<https://bioinformatics.csic.es/tools/venny/index.html>) was utilized to collect the coincident targets shared between biologically active constituents of WSF and NAFLD-associated targets which were regarded as prospective targets of WSF to ameliorate NAFLD. The STRING database (<https://string-db.org>, version 12.0) was employed to build the PPI networks with constraints of a medium confidence threshold of 0.400 and homo sapiens. Subsequently, the resulting data was submitted to Cytoscape 3.7.1 for visualization purposes. Core targets were further discerned through the topological analysis of the CentiScaPe 2.2 plug-in in terms of parameters like betweenness, closeness and degree.

Gene ontology (GO) function and Kyoto encyclopedia of genes and genomes (KEGG) enrichment analysis

The intersecting targets derived above were uploaded into DAVID database (<https://david.ncifcrf.gov>, v2024q2) for KEGG and GO enrichment analysis, encompassing biological process (BP), cellular component (CC) and molecular function (MF) analysis. In the KEGG analysis, pathways with less than 0.05 *P*-values and their accordant enriched targets were selectively retained to identify crucial pathways and pivotal targets related to the impact of WSF on NAFLD. Finally, Weishengxin (<http://www.bioinformatics.com.cn>) was utilized for visualization purposes of the top 20 BP and KEGG pathway results according to gene counts or ratios in bubble and bar graphs.

Molecular docking

The bioactive components with degree values ≥ 10 in the “active components-target-pathway” network were regarded as ligands in subsequent molecular docking analysis. The 2D structure of aforesaid components were

obtained from the PubChem database (<https://pubchem.ncbi.nlm.nih.gov>), while the 3D structures with minimum energy were drawn through Chem3D software. The protein structure database Protein Data Bank database (<http://www.rcsb.org>) was utilized to retrieve the structural details about the core targets in inflammation related pathways with restrictions of homo sapiens, X-ray diffraction, refinement resolution ≤ 2.5 Å. The water molecules and original ligand structures in the selected proteins were removed, as well as hydrogen atoms were added by PyMoL software. Subsequently, molecular docking explorations were conducted to evaluate the optimal semi-flexible binding modes with retained rotatable bonds of the biochemicals by using the AutoDock Vina with Vina default force field and scoring function (Trott and Olson 2010).

In an effort to improve the precision of molecular docking predictions, we conducted additional flexible docking simulations. Building upon the minimum binding energy conformation derived from a semi-flexible docking protocol, we designated amino acid residues within a 5 Å sphere centered on the ligand as flexible, permitting free rotation of their side chains. AutoDock Vina was then re-employed for docking, and conformations exhibiting intramolecular hydrogen bonds were discarded.

To determine the final ranking, we calculate the sum of the rankings of the lowest binding energies of a certain molecule to all proteins firstly, and then sort the numerical values of the ranking sums of all molecules in ascending order. Ultimately, the hydrogen bond linkage with protein residues of the top two optimal biomolecules with the minimum binding energy ranking were visualized by PyMoL software.

Immunohistochemistry (IHC) analysis of related proteins in the liver

The expression and localization of Toll-like receptor 4 (TLR4), nuclear factor-kappa B (NF- κ B), cyclooxygenase 2 (COX-2) and interleukin-6 (IL-6) in the liver were determined by IHC analysis. The procedures for IHC staining were comparable to we described previously (Li et al. 2019a, b). In brief, the tissue slices were subjected to procedural deparaffinization, antigen retrieval with citrate buffer liquid (pH 6.0), incubation with appropriate primary antibodies (1:200 dilution) and HRP-conjugated secondary antibodies in turn, respectively. Subsequently, the positive expression signals were visualized under the optical microscope via DAB staining in yellow color, while the nuclei underwent counterstaining with hematoxylin. The protein expression data were subjected to semi-quantitative analysis through the computation of integrated optical density (IOD) values within the positively stained areas of microphotographs with the

Image-Pro Plus software (version 6.0). The catalog and lot numbers of utilized antibodies are included in supplementary file.

ELISA determination of inflammation factors in the liver

The liver tissues were precisely weighed with the subsequent addition of an equivalent volume of saline solution at a 1:10 (w/v) ratio and thorough mixing. Then, the supernatants schemed for the following trails were subjected to homogenization and centrifugation at 12,000 rpm from the resultant mixtures above at 4 °C for 10 min. In final, the mouse ELISA kits of tumor necrosis factor α (TNF- α) and interleukin-1 β (IL-1 β) were utilized for their concentration determination in the liver as per the provided instructions.

Western blot (WB) analysis of related proteins in the liver

In short, precisely weighted liver tissue was lysed in the RIPA buffer containing protease inhibitor and EDTA (100:1:1, v/v/v) at 4 °C with subsequent homogenate centrifugation for 10 min to get supernatants at 12,000 rpm for further WB analysis, prior to the concentration's detection of total protein via the BCA assay kit. After being degenerated with loading buffer at 95 °C, protein samples were isolated via 10% SDS-PAGE under conditions of 80 V for 30 min, followed by 120 V for 90 min and subsequently electrotransferred onto a nitrocellulose membrane in ice (200 mA with TLR4: 90 min, NF- κ B and COX2: 60 min, β -actin: 40 min). Membranes were then blocked at room temperature with protein-free rapid blocking buffer for 20 min, followed by overnight incubation with respective primary antibodies (TLR4 1:1000, NF- κ B 1:1000, COX-2 1:750, dilution) at 4 °C. β -actin (1:1000, dilution) was served as the loading control. After a 1-h incubation with paired HRP-conjugated secondary antibodies, the protein bands were visualized via an enhanced chemiluminescent detection system (ChemScope 6000, CLINX, China). The semi-quantification of gauging protein expressions was standardized against β -actin densitometry conducted with ImageJ software (version 1.53K).

Statistical analysis

All data were presented as the average values \pm standard deviation (SD). Statistical analyses entailed one-way analysis of variance (ANOVA), supplemented with Tukey's honest significant difference (HSD) test for intergroup comparisons. A statistical significance threshold was set at $P \leq 0.05$. All analyses of statistics were performed through an updated version of SPSS software. Diagram visualization was implemented by GraphPad Prims.

Results

WSF attenuated body weight and visceral fat accumulation

Animal experiment procedures are shown in Fig. 1A. The body weight of the MC mice increased significantly since modeling since the 5th weeks compared with the NC group ($P < 0.05$) (Fig. 1B). And after modeling for 17 weeks, the weight gain, liver mass, and epididymal adipose (EA) mass of the MC mice also increased significantly ($P < 0.01$) (Fig. 1C–E). PPC, a key component of essential phospholipids renowned for its efficacy in treating NAFLD, is instrumental in preserving hepatic cell membrane fluidity and functionality (Lu et al. 2022). Compared to the MC group, the body weight of the PPC and WS mice decreased significantly, starting from the 5th and 7th weeks of PPC and WSF administration ($P < 0.01$), respectively (Fig. 1B). Besides, the weight gain, EA mass and its index of the PPC and WS mice decreased ($P < 0.01$), while PPC has no obvious effect on EA index (Fig. 1C–G). These results indicated that WSF treatment could reverse abnormal weight gain and visceral fat accumulation caused by the HSHF diet.

WSF improved liver function and pathological lesions

After modeling for 17 weeks of the HSHF diet, the serum levels of AST and ALT in the MC mice increased significantly compared with the NC group ($P < 0.01$) (Fig. 2B, C). The H&E and Oil Red O staining demonstrated an increase of inflammatory foci (indicated by arrowheads),

extensive hepatocyte ballooning lesions, and aberrant lipid accumulation in the liver of NAFLD mice (Fig. 2A, E). Besides, the NAS score of the MC mice also increased significantly ($P < 0.01$) (Fig. 2D), demonstrating that the normal physiological structure of the liver was severely damaged. Compared with the MC group, PPC and WSF could lessen the levels of serum AST and ALT significantly ($P < 0.01$) (Fig. 2B, C). Meanwhile, the inflammatory cell infiltration was reduced and other pathological changes of the liver were reversed as attested by H&E and Oil Red O staining (Fig. 2A). In addition, the NAS score and Oil Red O area ratio decreased in various degrees ($P < 0.05, 0.01$) (Fig. 2D, E). Collectively, these results showing that WSF improved liver function and attenuated pathological lesions of inflammatory and steatosis.

WSF ameliorated lipid metabolism

In divergence from the NC group, the levels of serum TC, TG, LDL-c as well as liver TC, TG in the MC mice increased significantly ($P < 0.01$) (Fig. 3A, B, D–F), while serum HDL-c levels decreased obviously ($P < 0.01$) (Fig. 3C) after modeling for 17 weeks, suggesting that there might be abnormal lipid metabolism in HSHF diet-induced NAFLD mice. Compared with the MC group, PPC and WSF treatment could suppress the increase of serum TG and liver TG and the decrease of serum HDL-c in various degrees ($P < 0.05, 0.01$), but had no effect on serum TC and LDL-c (Fig. 3A–F). Moreover,

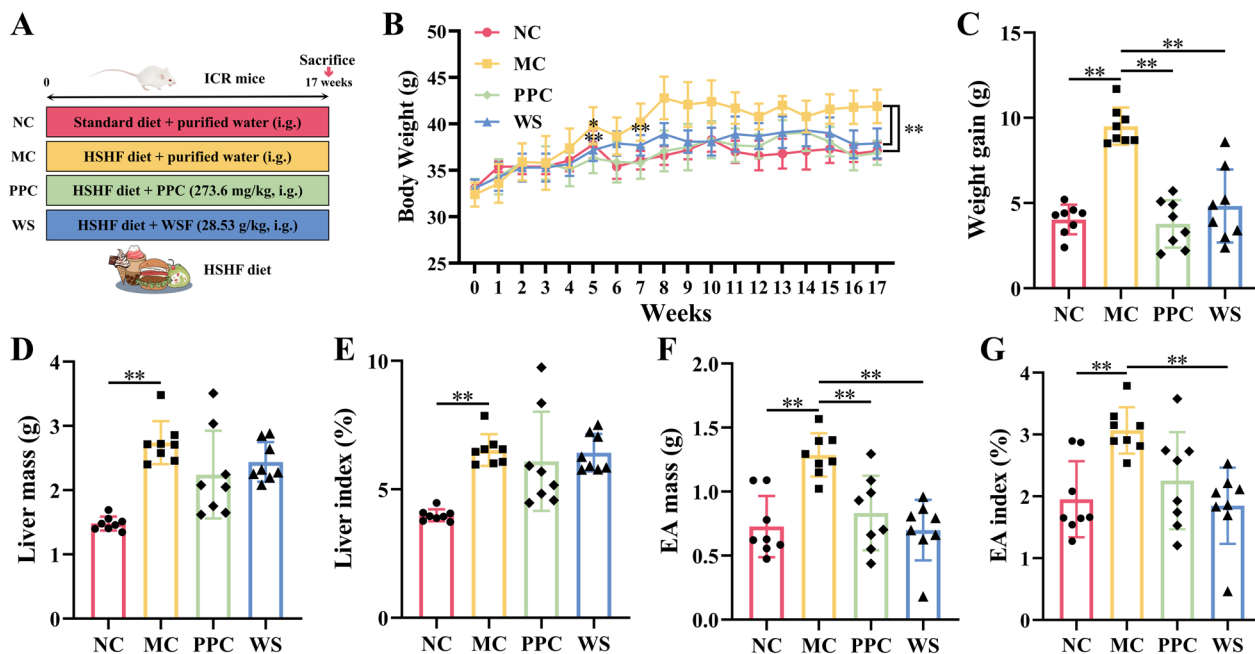


Fig. 1 Effects of WSF on body weight and visceral fat accumulation. **A** Animal experiment procedures. **B** Body weight change during the whole experiment. **C** Weight gain. **D** Liver mass. **E** Liver index. **F** Epididymis adipose mass. **G** Epididymis adipose index. All values were presented as mean \pm SD with significance markers of * $P < 0.05$ and ** $P < 0.01$

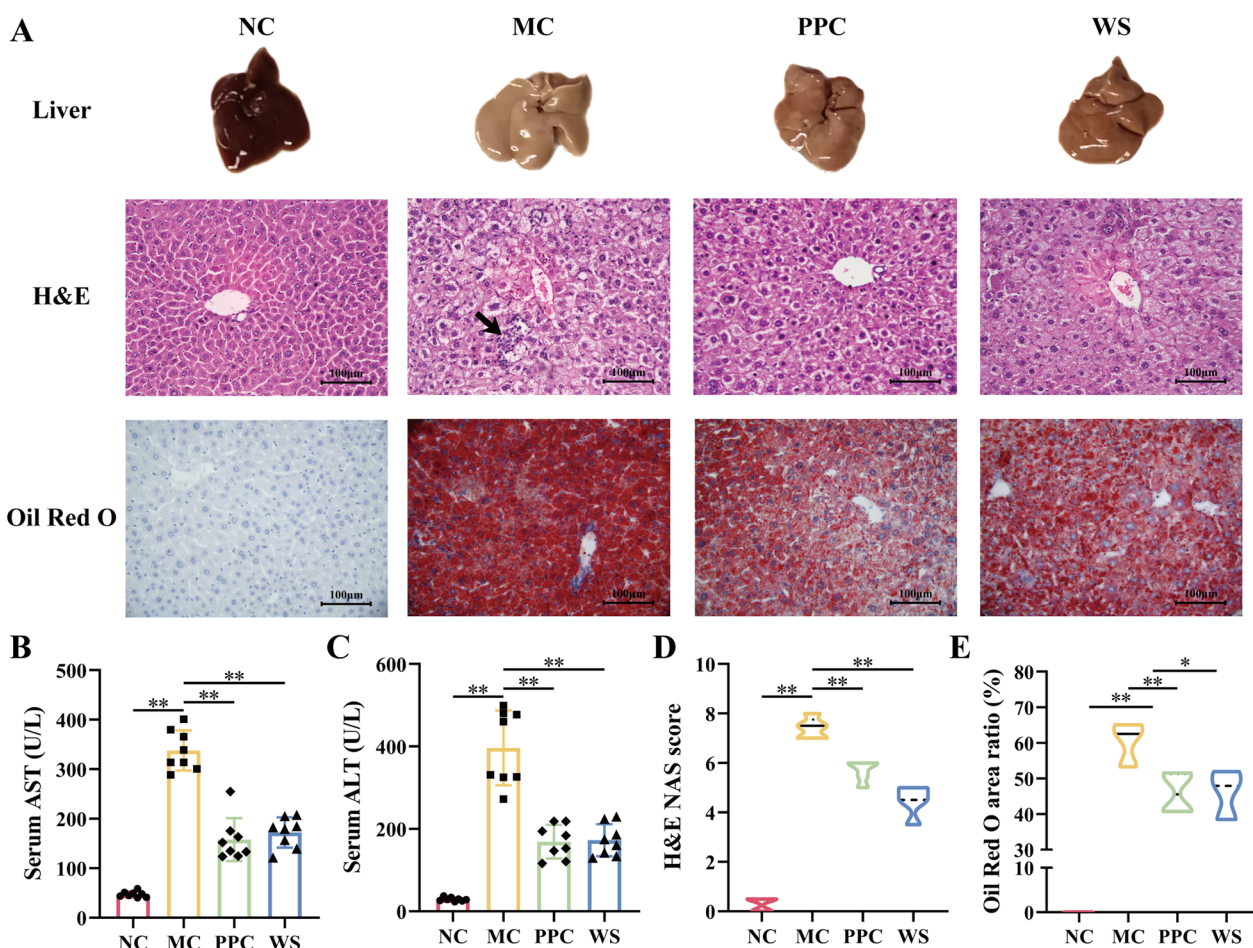


Fig. 2 Effects of WSF on liver function and hepatic pathology. **A** Representative graphs of morphology and pathological changes in liver (H&E 400×; Oil Red O 400×). **B** Serum AST. **C** Serum ALT. **D** NAFLD activity scores. **E** Oil Red O staining area ratio. All values were presented as mean ± SD with significance markers of * $P < 0.05$ and ** $P < 0.01$

we observed that after 17 weeks of modeling, there was a trend towards elevated serum GLU levels in MC mice (without significant difference), whereas administration of PPC and WSF could normalize the serum GLU levels. These results suggested that WSF could ameliorated and lipid metabolism disorder induced by NAFLD through regulating the serum levels of TG and HDL-c and TG accumulation in the liver.

Identification of phytochemical components in WSF

The Agilent HPLC-Q-TOF/MS system was exploited to evaluate phytochemical components of WSE, and total ion chromatogram profiles were acquired via full scan under both positive and negative electrospray ionization modes (Fig. 4). In comparison with the HMDB, MassBank, TCMSP databases and data from related literature searched from CNKI, Wanfang and VIP databases, 39 potential compounds were tentatively recognized in accordance with their retention time (RT), molecular

formulas, differences in theoretical and observed quasi-molecular ion mass (m/z), errors in ppm, scores of Agilent Masshunter and MS/MS fragment ion circumstances in total. Wherein, 7 kinds of mutual compounds were identified simultaneously in positive and negative modes. The majority of the detected components were attributed to flavonoids (including flavone glycosides), alkaloids, phenylpropanoids (including coumarins and lignans) and phenolic acids. The specific information of components identified tentatively in WSF was listed in Table 2.

Bioinformatics-based analysis

Acquisition of WSF component targets and NAFLD disease targets

A total of 72 chemical components from WSF were acquired from the HPLC-Q-TOF/MS results, TCMSP database and literature search after Swiss ADME platform screening. Subsequently, 878 protein targets for the 72 active ingredients present in WSF were identified by

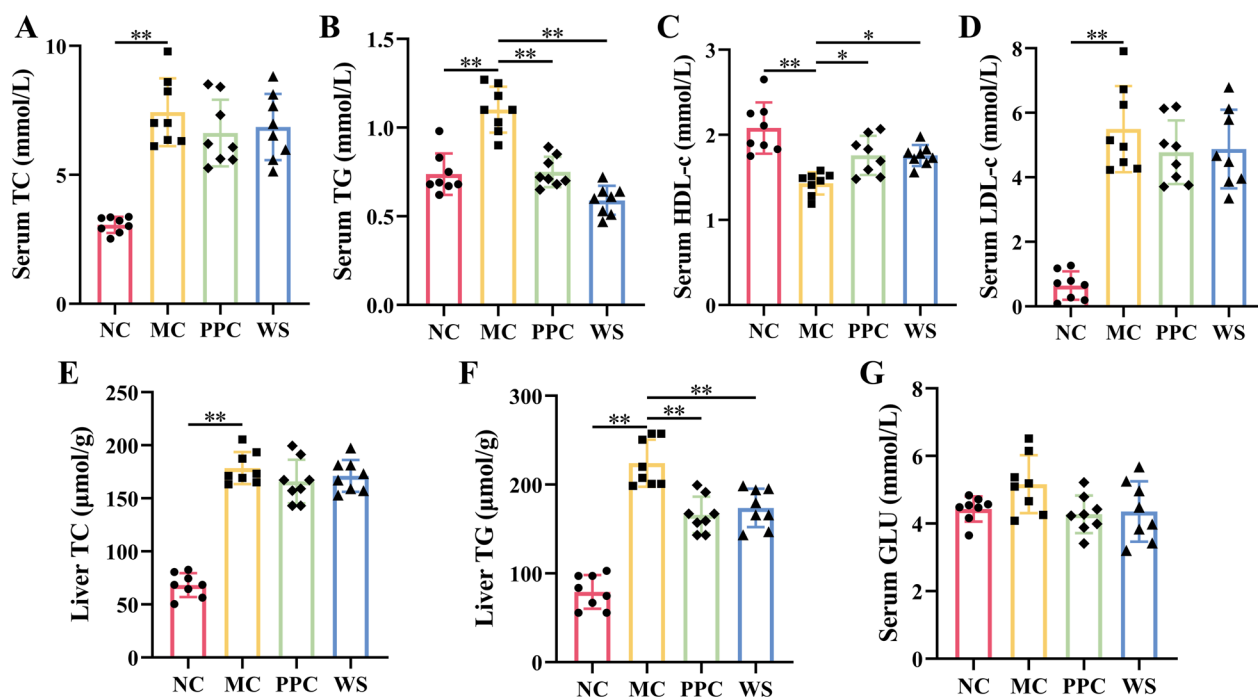


Fig. 3 Effects of WSF on glycolipid metabolism. **A–D** Levels of TC, TG, HDL-c, and LDL-c in serum. **E, F** Levels of TC and TG in liver. **G** Levels of GLU in serum. All values were presented as mean \pm SD with significance markers of * $P < 0.05$ and ** $P < 0.01$

using the Swiss Target Prediction platform after removing repetitive targets with their canonical SMILES. After deduplication, a total of 1573 unique NAFLD-related targets were compiled from a combination of the GeneCards, DisGENET and OMIM databases, which were used as disease targets of NAFLD for later analysis. The Venny 2.1.0 website was further subjected to coincide targets associated with the WSF with the NAFLD disease-related targets, yielding 254 shared targets in total as prospective therapeutic targets for the NAFLD treatment by the WSF (Fig. 5A).

Construction of the herbs-active components-targets network map

Cytoscape 3.7.1 was utilized to construct an interaction map of the herbs-active components-targets network, consisting of 338 nodes and 2037 edges (Fig. 5B). The nodes in the network were distinguished by size, which had a positive correlation with the degree values. The map was further subjected to additional topological analysis across “Network analyzer” tool. Topological results implied that the centralization of the network is 0.135 and the heterogeneity is 1.033, while the average CNC is 0.35, showing that some nodes in the network were more concentrated and contributive than others. The average degree of the network is 12.05, and there are 63 component nodes and 55 target nodes above this value. The

gypentonoside A_{qt} node has the highest degree value with connections to 56 targets, and the target CYP19A1 is connected to 46 components of WSF. It is indicated that bioactive components could interact with singular or multiple targets, while various components might also share common targets. Collectively, these insights propose a multi-component and multi-target mode of action for WSF in eliciting complex pathophysiological alterations pertinent to NAFLD therapy. Details of components in WSF that ranked within the top 10 based on their degree values were listed in Table 3.

Construction of the PPI network map

To further investigate the therapeutic mechanisms of WSF on NAFLD, PPI analysis of the coincident targets was implemented with the STRING database. The original PPI network comprised 253 nodes interconnected by 4943 edges with a degree value of 39.075 on average and a clustering coefficient of 0.547 on average, which characterized the intricate protein interaction collectively. Utilizing the CentiScaPe 2.2 plugin for topological analysis, the processed PPI network was subsequently visualized through Cytoscape 3.7.1 software (Fig. 5C), employing stringent selection criteria of degree > 39.075 , betweenness centrality > 251.65 , and closeness centrality > 0.002 to discern top 50 key genes. The brighter color and larger size of circles were positive correlation with the degree

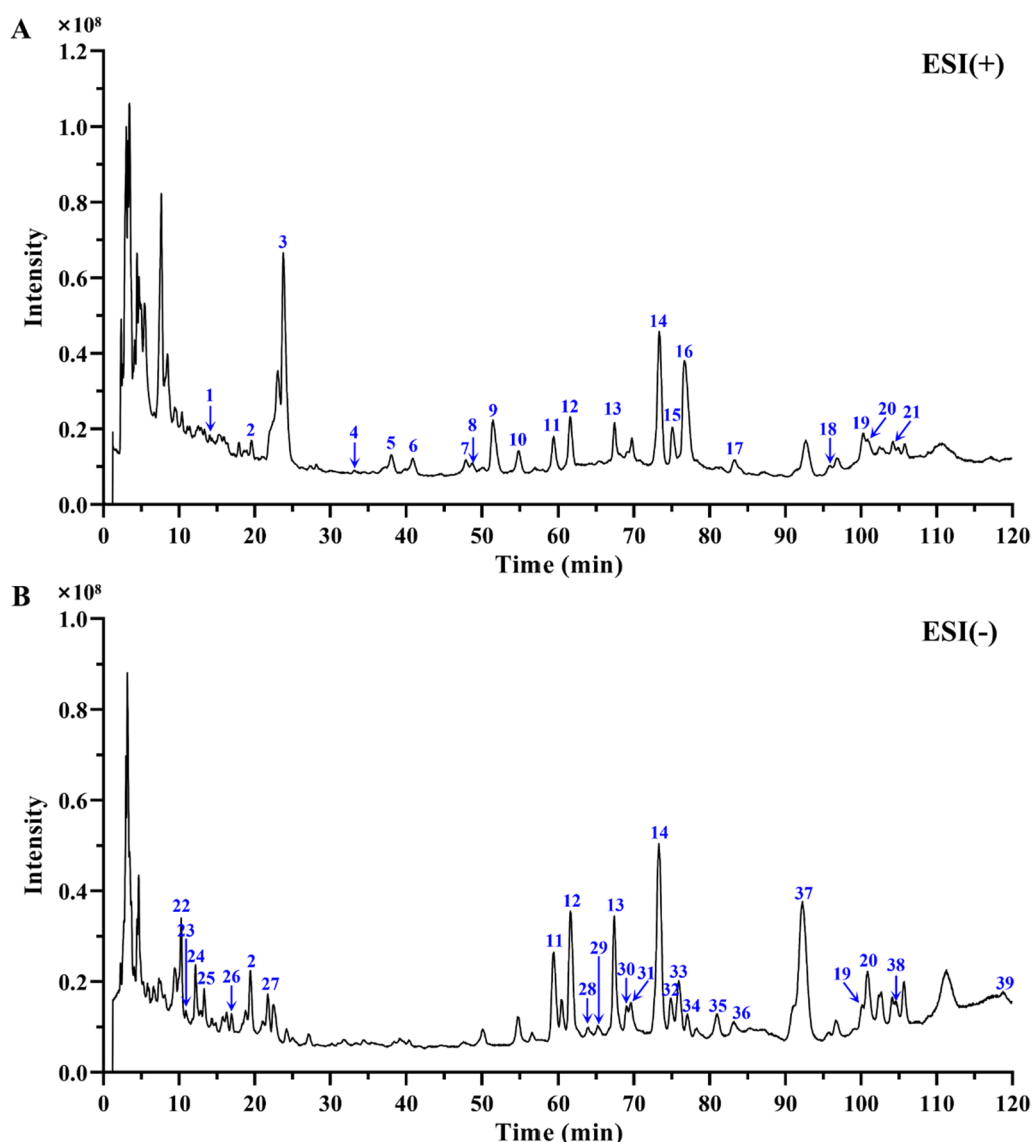


Fig. 4 The total ion chromatogram (TIC) profiles in positive (A) and negative ion mode (B). Peaks 1–39 correlate with the compounds enumerated in Table 2

values, while the thicker width and brighter color of edges were positive correlation with the combined score. In final, a total of 50 core targets with 873 edges were screened out, and TNF (162), IL6 (157), AKT1 (157), IL1B (142), and PPARG (136) were the top 5 targets according to their degree values, and PTGS2 also has a relatively high degree value of 109, which were all considered as the key anti-NAFLD targets of WSF.

GO and KEGG analysis

GO analysis of the coincident targets mutual to WSF and NAFLD was conducted via the DAVID database. The outcomes of GO analysis disclosed that BP-related

alterations were primarily in linkage with 882 functional annotations, comprising positive regulation of transcription from RNA polymerase II promoter, signal transduction, protein phosphorylation, inflammatory response (rank 10), and the response to lipopolysaccharide (LPS, rank 13), etc. (Fig. 6A). Wherein, LPS constitutes a primary composition of the outer membrane in Gram-negative bacterial cell walls and could participate in NAFLD inflammatory progression via activation of the gut-liver axis LPS/TLR4/NF- κ B pathway (Han et al. 2022). Besides, alterations related to CC primarily encompassed 97 functional annotations, with a substantial focus on locations of the cytosol, cytoplasm and plasma membrane etc.

Table 2 Identification of chemical compounds in WSF via HPLC-Q-TOF/MS

No	RT (min)	Putative compounds	Molecular formula	Observed m/z	Theoretical m/z	Error (ppm)	Score	ESI mode	CAS number
1	14.021	Higenamine	C ₁₆ H ₁₇ NO ₃	272.1273	271.1208	3.59	94.64	+	5843-65-2
2	19.589	Chlorogenic acid	C ₁₆ H ₁₈ O ₉	355.1011	354.0951	3.85	91.21	+	327-97-9
	19.404	Chlorogenic acid	C ₁₆ H ₁₈ O ₉	353.0879	354.0951	0.20	97.67	-	327-97-9
3	23.777	Sinapine	C ₁₆ H ₂₄ NO ₅	310.1642	310.1654	2.32	95.86	+	18696-26-9
4	33.151	Phenprobamate	C ₁₀ H ₁₃ NO ₂	180.1008	179.0946	6.05	93.81	+	673-31-4
5	38.053	(-)-Artemepavine	C ₁₉ H ₂₃ NO ₃	314.1745	313.1678	2.20	96.73	+	524-20-9
6	40.895	(-)-N-Methylcoclaurine	C ₁₈ H ₂₁ NO ₃	300.1589	299.1521	2.24	95.60	+	5096-70-8
7	47.909	Asimilobine	C ₁₇ H ₁₇ NO ₂	268.1323	267.1259	3.91	93.42	+	6871-21-2
8	48.757	Coclaurine	C ₁₇ H ₁₉ NO ₃	286.1435	285.1365	1.71	97.00	+	486-39-5
9	51.466	N-nornuciferine	C ₁₈ H ₁₉ NO ₂	282.1482	281.1416	2.61	97.28	+	3153-55-7
10	54.823	Calycosin 7-galactoside	C ₂₂ H ₂₂ O ₁₀	447.1280	446.1213	1.77	96.77	+	114272-30-9
11	59.310	Rutin	C ₂₇ H ₃₀ O ₁₆	611.1598	610.1534	2.00	94.97	+	153-18-4
	59.310	Rutin	C ₂₇ H ₃₀ O ₁₆	609.1455	610.1534	1.28	97.92	-	153-18-4
12	61.570	Quercituron	C ₂₁ H ₁₈ O ₁₃	479.0810	478.0747	2.56	95.12	+	22688-79-5
	61.652	Quercituron	C ₂₁ H ₁₈ O ₁₃	477.0671	478.0747	1.09	98.32	-	22688-79-5
13	67.404	Naringin	C ₂₇ H ₃₂ O ₁₄	581.1857	580.1792	1.90	96.19	+	10236-47-2
	67.369	Naringin	C ₂₇ H ₃₂ O ₁₄	579.1712	580.1792	1.57	97.49	-	10236-47-2
14	73.321	Hesperidin	C ₂₈ H ₃₄ O ₁₅	611.1960	610.1898	1.96	96.28	+	520-26-3
	73.269	Hesperidin	C ₂₈ H ₃₄ O ₁₅	609.1818	610.1898	1.48	97.56	-	520-26-3
15	75.082	O-nornuciferine	C ₁₈ H ₁₉ NO ₂	282.1482	281.1416	2.61	97.28	+	3153-55-7
16	76.695	(-)-Nuciferine	C ₁₉ H ₂₁ NO ₂	296.1638	295.1572	3.23	95.11	+	475-83-2
17	83.243	Ononin	C ₂₂ H ₂₂ O ₉	431.1322	430.1264	3.83	89.01	+	486-62-4
18	95.807	Methylnissolin	C ₁₇ H ₁₆ O ₅	301.1055	300.0998	5.57	87.22	+	73340-41-7
19	100.261	Wogonin	C ₁₆ H ₁₂ O ₅	285.0750	284.0685	3.14	95.60	+	632-85-9
	100.110	Wogonin	C ₁₆ H ₁₂ O ₅	283.0613	284.0685	0.26	97.79	-	632-85-9
20	100.943	Quercetin	C ₁₅ H ₁₀ O ₇	303.0492	302.0427	2.89	95.01	+	117-39-5
	100.841	Quercetin	C ₁₅ H ₁₀ O ₇	301.0353	302.0427	0.62	98.27	-	117-39-5
21	104.200	Poncirin	C ₂₈ H ₃₄ O ₁₄	595.2003	594.1949	3.52	88.63	+	14941-08-3
22	10.280	Danshensu	C ₉ H ₁₀ O ₅	197.0457	198.0528	-0.65	98.48	-	42085-50-7
23	10.895	Vanillic acid	C ₈ H ₈ O ₄	167.0351	168.0423	-0.48	98.74	-	121-34-6
24	12.161	Protocatechuic acid	C ₇ H ₆ O ₄	153.0195	154.0266	-0.82	86.79	-	99-50-3
25	13.305	Neochlorogenic acid	C ₁₆ H ₁₈ O ₉	353.0877	354.0951	0.80	97.77	-	906-33-2
26	16.928	Protocatechualdehyde	C ₇ H ₆ O ₃	137.0246	138.0317	-0.73	99.29	-	139-85-5
27	21.731	Cryptochlorogenic acid	C ₁₆ H ₁₈ O ₉	353.0877	354.0951	0.65	97.38	-	905-99-7
28	63.845	Triphasiol	C ₁₉ H ₂₄ O ₆	347.1493	348.1573	2.48	94.09	-	81445-98-9
29	65.241	Carinol	C ₂₀ H ₂₆ O ₇	377.1592	378.1679	4.04	92.22	-	58139-12-1
30	68.998	Azelaic acid	C ₉ H ₁₆ O ₄	187.0977	188.1049	-0.12	98.67	-	123-99-9
31	69.612	Astragalin	C ₂₁ H ₂₀ O ₁₁	447.0921	448.1006	2.55	44.64	-	480-10-4
32	74.831	Paramiltioic acid	C ₁₉ H ₂₄ O ₅	331.1549	332.1624	0.91	98.82	-	140396-85-6
33	75.928	Rosmarinic acid	C ₁₈ H ₁₆ O ₈	359.0774	360.0845	0.19	98.15	-	20283-92-5
34	76.992	Marmin	C ₁₉ H ₂₄ O ₅	331.1551	332.1624	0.55	98.30	-	14957-38-1
35	80.964	Salvianolic acid A	C ₂₆ H ₂₂ O ₁₀	493.1145	494.1213	0.16	96.16	-	96574-01-5
36	84.687	Isorhamnetin	C ₁₆ H ₁₂ O ₇	315.0516	316.0583	-0.84	96.37	-	480-19-3
37	92.215	Salvianolic acid B	C ₃₆ H ₃₀ O ₁₆	717.1455	718.1534	0.99	97.51	-	121521-90-2
38	104.564	Monomethyl lithospermate	C ₂₈ H ₂₄ O ₁₂	551.1190	552.1268	1.69	95.46	-	933054-33-2
39	118.009	Ombuin	C ₁₇ H ₁₄ O ₇	329.0670	330.0740	-0.28	97.70	-	552-54-5

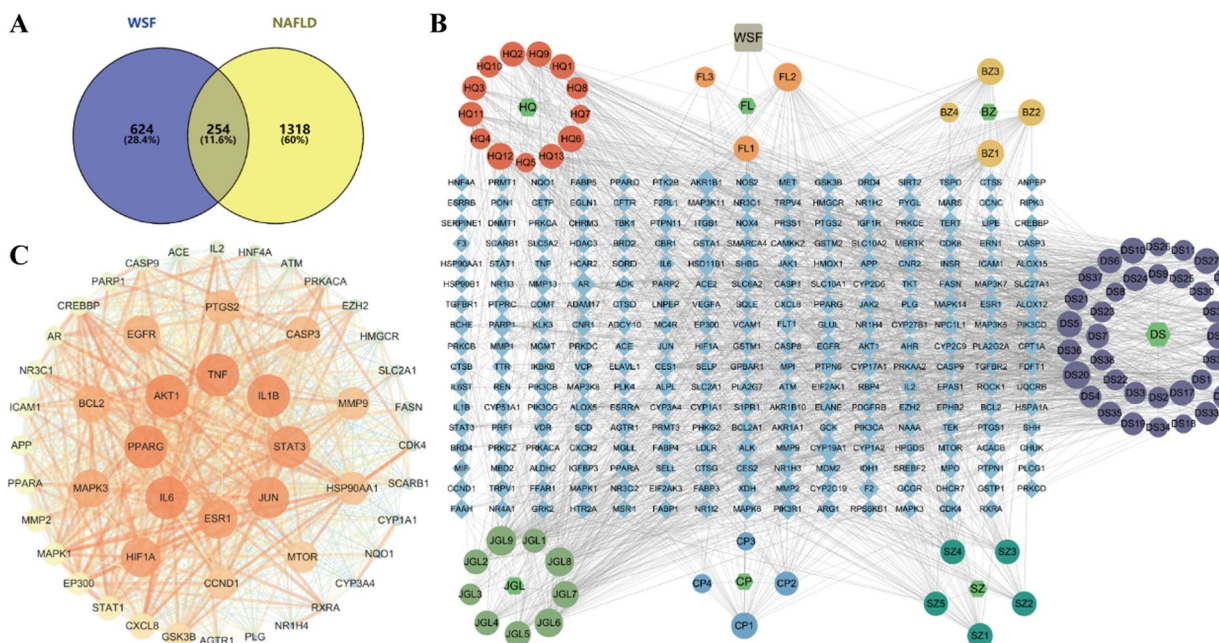


Fig. 5 Analysis of core components and proteins for WSF on NAFLD treatment. **A** Venn diagram of targets. **B** Herbs-active components-targets network. **C** PPI network of core targets possessing the highest 50-degree values

And the majority of alterations related to MF were predominantly characterized by 208 functional annotations, encompassing protein binding, identical protein binding and ATP binding, etc. The CC and MF outcomes of GO analysis were not visualized in this article.

The coincident targets between WSF and NAFLD were also submitted to the DAVID database for an in-depth analysis of the KEGG, and the 156 related pathways were screened with a criterion of $P < 0.01$. The enrichment bar chart of the top 20 key pathways was drawn according to gene counts using Weishengxin website (Fig. 6B). Wherein, we found that pathways in cancer, metabolic pathways and lipid and atherosclerosis have the top 3 largest gene counts.

In accordance with PPI analysis results, we discovered that core proteins like TNF, IL6, IL1B and PTGS2 (COX2) were canonical pro-inflammatory cytokines. Moreover, the BP results also revealed the potential of WSF to ameliorate NAFLD by modulating inflammatory responses. Therefore, we conducted an in-depth exploration of the KEGG analysis results and found that inflammation related pathways like TNF, IL-17, Toll-like receptor and NF-kappa B signaling pathway were also involved in enrichment pathways with gene counts ≥ 15 (Fig. 6C). These selected 4 pathways (in brown gray) involved 41 related targets (in blue) and 67 chemical components (in green) with 112 nodes and 408 edges (Fig. 6D). In conclusion, the combination results of KEGG and PPI analysis indicated that WSF might act on NAFLD through

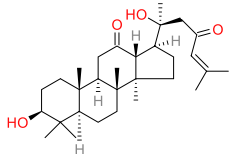
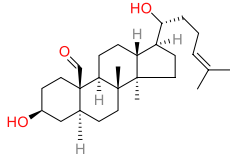
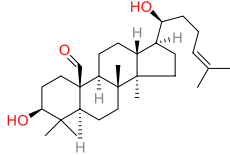
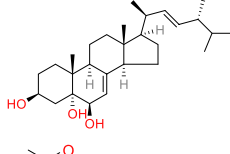
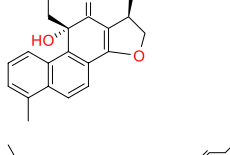
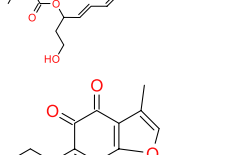
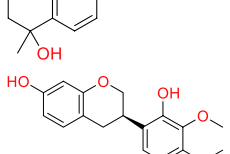
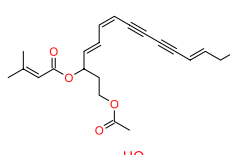
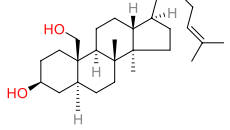

proteins in inflammation related pathways above, which would be validated with further experiments later.

Molecular docking

For the further affinity verification, molecular docking was carried out of the core proteins in inflammation related pathways (TLR4, NF- κ B, COX-2, IL-1 β , IL-6, and TNF- α) with 13 active components of degree values ≥ 10 in the “active components-target-pathway” network. The respective minimum binding energies between various active components with their CAS numbers and proteins with their PDB IDs were listed in Table 4. Furthermore, a heat map was constructed according to the minimum binding energy for intuitive visualization purpose (Fig. 7A). The stability of the ligand-receptor binding was inversely proportional to the binding energy, which indicated that a more stable interaction resulted in lower binding energy. It is considered to have a good affinity between ligands and receptors if the binding energy is below -5.0 kcal/mol (Jiang et al. 2022).

Our results implied that all the minimum binding energies were no more than -5.0 kcal/mol with a value of -7.17 kcal/mol on average, which indicated that most of the selected chemical components of WSF were conjugated tightly with pivotal proteins in inflammation related pathways. These data further proved that WSF might exert pharmacological effects against NAFLD by mediating the activities of inflammatory related proteins of the TLR4/NF- κ B/COX-2 pathway at the

Table 3 The information of components in WSF possessing the highest 10-degree values

Component name	Molecular formula	2D structure	Degree	ASPL	BNC	CNC
Gypentonoside A qt	C ₃₀ H ₄₈ O ₄		57	2.448	0.045	0.408
Gypenoside XXVIII qt	C ₂₇ H ₄₄ O ₃		53	2.478	0.037	0.404
Gypenoside XXXV qt	C ₂₉ H ₄₈ O ₃		52	2.484	0.031	0.403
Cerevisterol	C ₂₈ H ₄₆ O ₃		51	2.531	0.052	0.395
Danshenol A	C ₂₁ H ₂₀ O ₄		48	2.555	0.035	0.391
12-senecioid-2E,8E,10E-atractylentriol	C ₁₉ H ₂₂ O ₄		45	2.537	0.040	0.394
Przewaquinone c	C ₁₈ H ₁₆ O ₄		45	2.519	0.041	0.397
(3R)-3-(2-hydroxy-3,4-dimethoxyphenyl)chroman-7-ol	C ₁₇ H ₁₈ O ₅		43	2.596	0.024	0.385
14-acetyl-12-senecioid-2E,8Z,10E-atractylentriol	C ₂₀ H ₂₂ O ₅		43	2.543	0.032	0.393
Gypenoside XXVII qt	C ₂₇ H ₄₆ O ₃		43	2.531	0.030	0.395

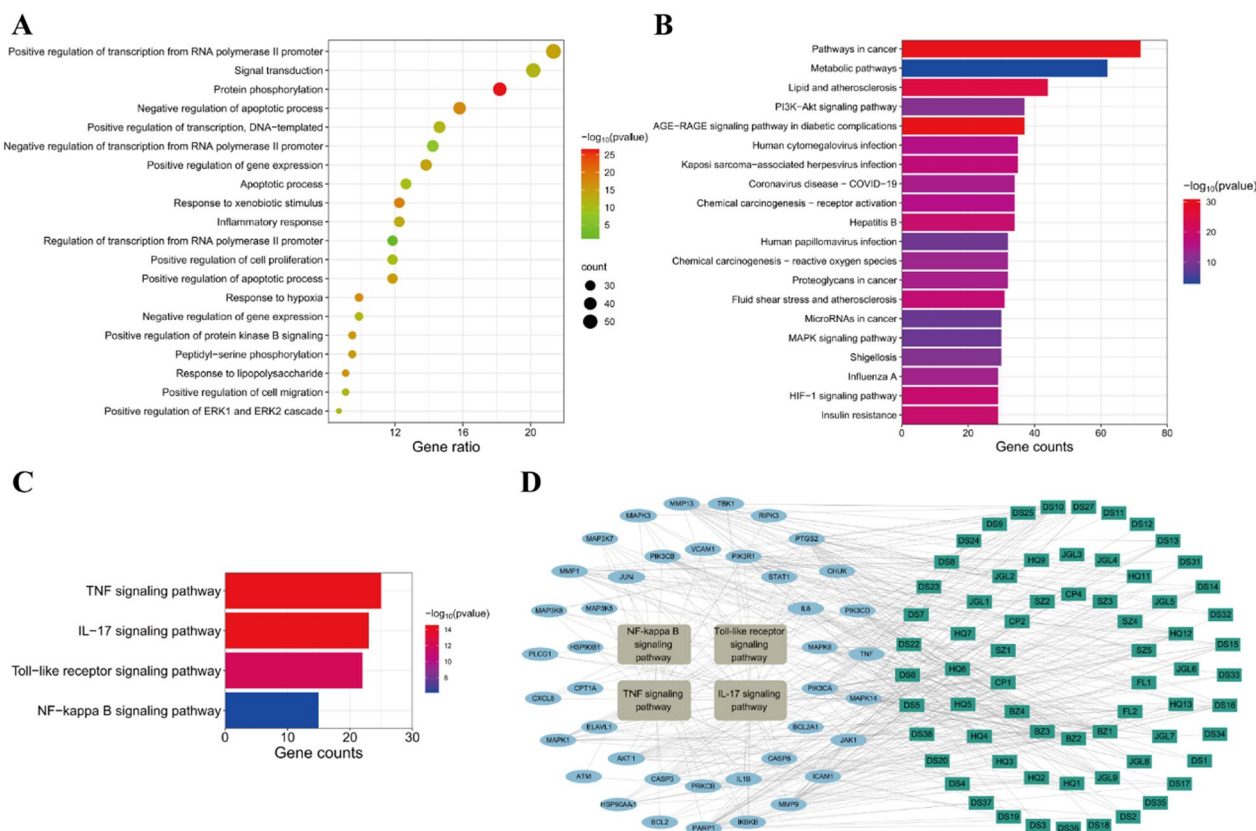


Fig. 6 Enrichment analysis for WSF on NAFLD treatment. **A** BP results of GO analysis (top 20). **B** KEGG pathway analysis results (top 20). **C** Analytical results of selected pathways. **D** Active components-target-pathway network of WSF on treating NAFLD

molecular conformation level. Besides, we found that JGL5 (gypenoside XXXVI), JGL8 (gypenoside XXVIII), FL1 (16 α -hydroxydehydrotrametenolic acid), JGL9 (gypentonoside-A) and JGL6 (gypenoside XXXV) have lower minimum binding energies to almost all core targets, indicating that they might be the core components of WSF in NAFLD therapy. Representative simulation figures of core protein-active component docking patterns were drawn by PyMol software with links between certain binding residue positions and hydrogen bonds (Fig. 7B–D).

Effects of WSF on the critical protein expressions and inflammatory factor levels in the liver

To further validate the anti-NAFLD effect of WSF across the inflammatory TLR4/NF- κ B/COX-2 pathway in diet-induced mice, IHC (Fig. 8A), WB (Fig. 9A) and ELISA analyses of pivotal proteins and inflammation factors in the liver were performed. Compared to the NC group, the HSHF diet would induce an increase in levels of TLR4, NF- κ B and COX-2 expression in NAFLD mice livers ($P < 0.05, 0.01$) (Fig. 8B–D, Fig. 9B) and promote the release of inflammation factors like IL-1 β , IL-6 and

TNF- α ($P < 0.05, 0.01$) (Fig. 8E–G). In contrast, intervention with WSF for 17 weeks could result in the diminution expression of TLR4, NF- κ B and COX-2 ($P < 0.05, 0.01$) (Fig. 8B–D, Fig. 9B) with reversed pro-inflammatory cytokine levels in the liver ($P < 0.01$) (Fig. 8E–G). These findings highlighted that WSF treatment indeed attenuated the NAFLD and inflammation in the liver across the TLR4/NF- κ B/COX-2 pathway, consistent with the results obtained above by the bioinformatics and molecular docking.

Discussion

NAFLD refers to a clinical syndrome pathologically characterized by inordinate intracellular lipid deposition in the liver due to factors other than alcohol and other well-defined hepatocyte-damaging elements, with a spectrum of diseases including NAFL, NASH, hepatic fibrosis, cirrhosis, or even hepatocellular carcinoma (HCC) (Chalasanani et al. 2018). Nowadays, the NAFLD incidence of the population in Asian countries is around 27.4%, with a continuous upward and younger trend (Fan et al. 2017; Anderson et al. 2015). NAFLD in children is characterized by rapid progression, 25.0%-50.0% have

Table 4 The respective minimum binding energy of components in WSF with core proteins

Active components	Minimum binding energy (kcal/mol)					
	TLR4 (2Z62)	NF-κB (1MY7)	COX-2 (5F19)	IL-1β (4NI7)	IL-6 (5R8E)	TNF-α (5UUI)
JGL5 (90058-55-2)	-8.0	-7.9	-12.7	-8.1	-6.6	-7.4
JGL8 (81474-80-8)	-8.2	-7.6	-11.0	-8.2	-6.4	-7.3
FL1 (176390-66-2)	-8.2	-7.6	-10.1	-7.7	-6.8	-7.1
JGL9 (187277-03-8)	-7.5	-7.3	-10.7	-7.7	-6.5	-7.6
JGL6 (90058-54-1)	-7.3	-8.4	-9.9	-8.0	-6.0	-7.4
DS27 (2237283-20-2)	-7.6	-7.4	-9.1	-7.3	-6.7	-7.1
DS16 (142694-58-4)	-7.4	-7.1	-8.2	-7.7	-6.8	-6.8
DS10 (135040-83-4)	-7.4	-6.1	-9.1	-6.6	-6.3	-6.6
HQ12 (64474-51-7)	-8.0	-6.1	-8.8	-6.5	-6.1	-6.3
DS15 (515-03-7)	-7.1	-5.9	-8.0	-6.2	-5.9	-6.0
BZ2 (113269-37-7)	-5.2	-5.3	-7.8	-6.6	-5.4	-5.6
BZ1 (113269-39-9)	-6.4	-5.5	-7.4	-5.5	-5.3	-5.6
BZ3 (113269-36-6)	-5.7	-5.0	-7.5	-5.8	-5.2	-5.3

developed NASH among confirmed cases of NAFLD in children, and 10.0%-25.0% have developed liver fibrosis as reported (Goyal and Schwimmer 2016). However, current used drugs mainly focused on weight loss, metabolism regulation, antioxidation and liver protection, and long-term application might induce increased risk of cancer, hemorrhagic stroke and symptomatic heart failure (Hsu et al. 2016). Therefore, there is still a lack of efficacious hepatoprotective medicine with few side effects, which seriously lowers the life quality of NAFLD patients of all ages.

TCM formulas often contain a variety of herbs with a myriad of active ingredients that could holistically modulate the intricate pathogenic network of NAFLD, as proven by long-term safe medication practices (Sun et al. 2021). In TCM theories, NAFLD was supposed to be a syndrome of deficient in origin and excessive in superficiality. Additionally, spleen deficiency was considered as Ben (primary aspect), while pathogenic factors like blood stasis and phlegm-dampness were Biao (secondary aspects) (Zhang et al. 2010). *Synopsis of the Golden Chamber* noted that “treating liver by nourishing spleen”, indicating that if the transportation function of spleen

was normal, qi and blood would be harmonized, and liver diseases could be cured as soon as possible (Wei et al. 2015). WSF was developed under the guidance of Prof. Wang Kun-Gen with the efficacy of “invigorating the spleen and benefiting the stomach, clearing heat and promoting diuresis”, which fits in with the above TCM theories of NAFLD treatment. Years of clinical experience have also proved that WSF performs well in managing metabolic diseases like hyperlipidemia and severe fatty liver (Shen et al. 2018). In summary, WSF has the potency for NAFLD prevention and treatment, but its modes of action need further systematic investigation. Therefore, we detect the pharmacological effects and relevant molecular pathways of WSF on NAFLD in this study.

According to expert consensus, dietary disorders (i.e., overeating of fat and sweets), more leisure with less labor, emotional disorders, physical weakness from prolonged illness and insufficient endowment were considered as the primary causes of NAFLD (Zhang and Li 2017). Epidemiology statistics also revealed that excessive sugar and lipid intake, which could increase the metabolic burden of the liver, were major risk factors

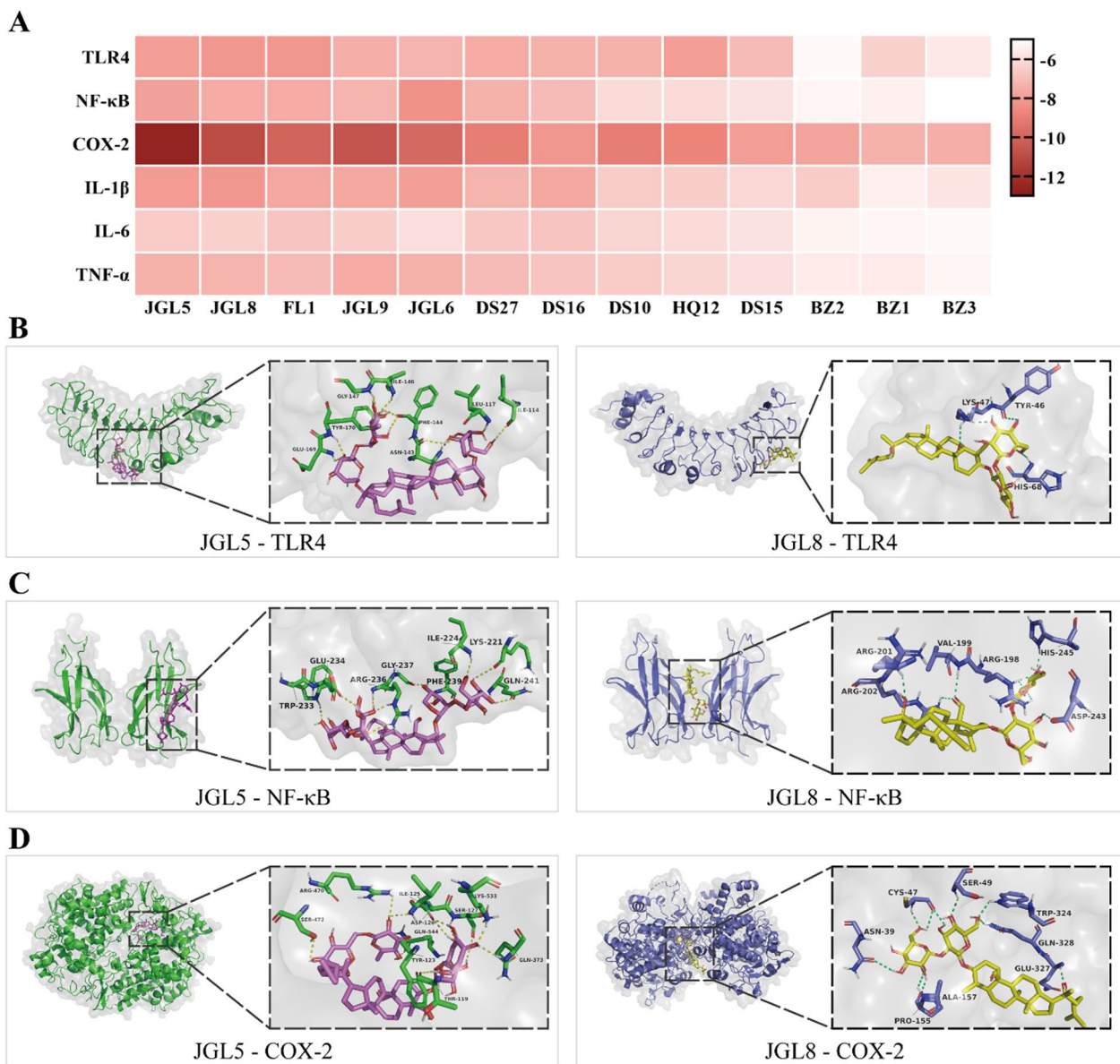


Fig. 7 Molecular docking results of ingredients in WSF with pivotal proteins. **A** Heat map in accordance with minimum binding energies. **B–D** The docking conformation of JGL5 and JGL8 with TLR4, NF-κB and COX-2

for NAFLD (Romero-Gómez et al. 2017). An increase in insulin resistance degree and hepatic fat storage is positively correlated with changes in plasma saturated fatty acids (Rosqvist et al. 2014). Moreover, excessive intake of sugar-sweetened beverages also has a positive correlation with fatty liver incidence and serum ALT levels (Ma et al. 2015). Therefore, the development of NAFLD models predominantly relies on dietary interventions with high-fat and high-sugar regimens to emulate the detrimental effects of an unhealthy human diet, except for drug-induced liver damage or unique strains of

animals (Fang et al. 2022). In this study, we found that the HSHF diet would induce typical symptoms of NAFLD similar to those in humans like obesity, lipid deposition in organs, increased transaminase levels, lipid metabolism disorder, hepatocellular degeneration and hepatic inflammatory cell infiltration, as reported in other studies (Chen et al. 2017; Porras et al. 2017).

In this study, we revealed a noteworthy therapeutic impact of WSF across multiple dimensions on NAFLD treatment. Obesity ranks as a primary risk factor in the development of NAFLD. Meta-analysis results illustrated

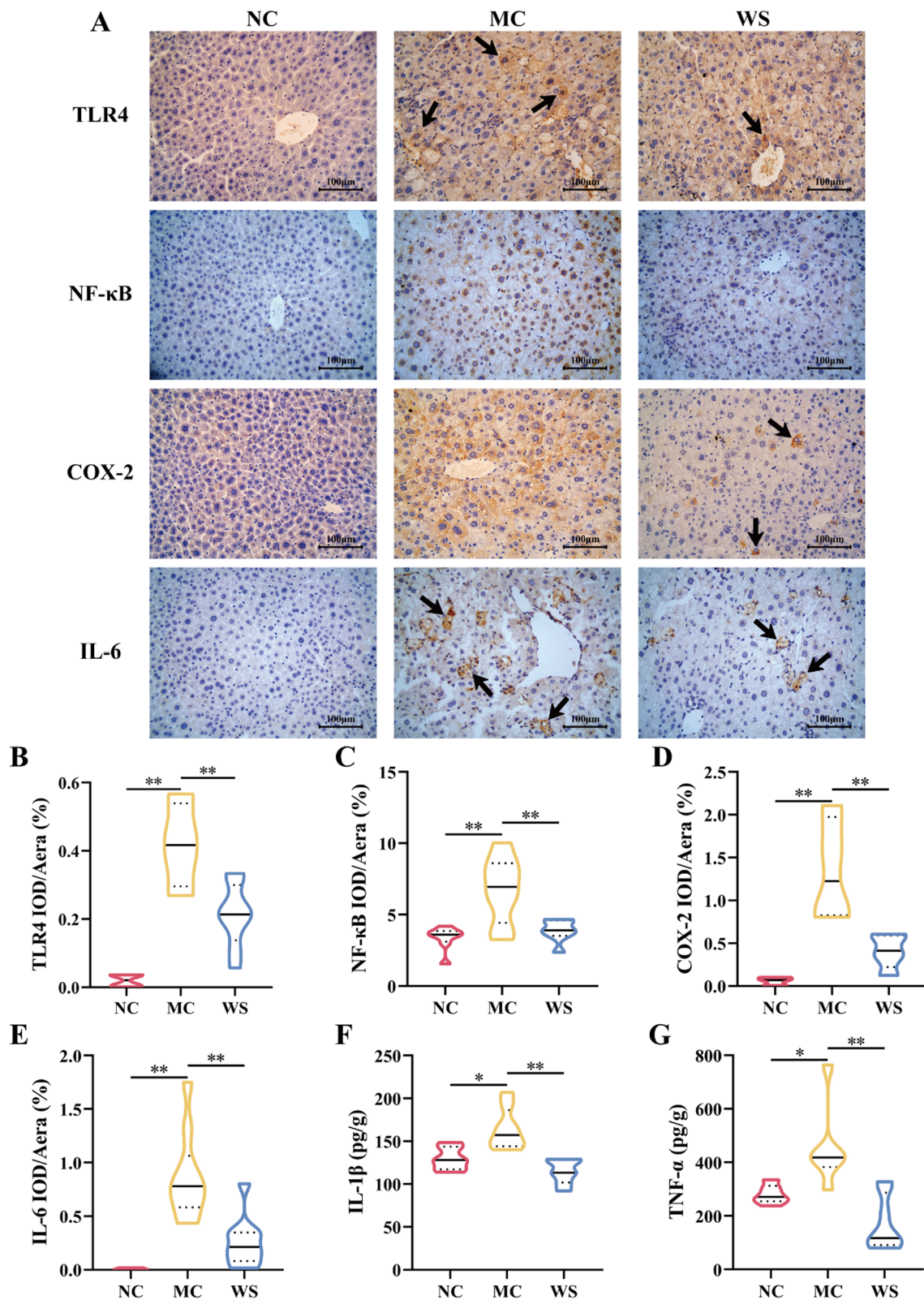


Fig. 8 Effects of WSF on liver inflammation via IHC and ELISA analysis. **A** IHC figures at the magnification of 400 ×. **B–E** Expression levels of TLR4, NF-κB, COX-2 and IL-6 in liver quantified by IHC assays. **F–G** Expression levels of IL-1β and TNF-α in liver quantified by ELISA assays. Black arrows refer to the positive expression sites of specific proteins. All values were presented as mean ± SD with significance markers of * $P < 0.05$ and ** $P < 0.01$

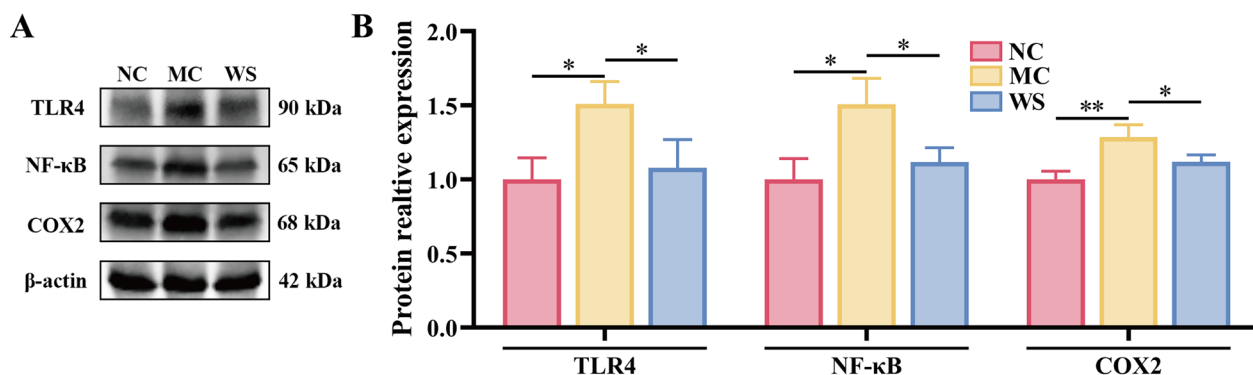


Fig. 9 Effects of WSF on hepatic inflammation via WB analysis. **A** Representative figures of WB. **B** Relative expression levels of TLR4, NF-κB and COX-2 to β-actin in the liver quantified by WB assays. All values were presented as mean ± SD with significance markers of * $P < 0.05$ and ** $P < 0.01$.

that 69.99% of individuals in the overweight category ($BMI \geq 25.0 \text{ kg/m}^2$) exhibited NAFLD prevalence, and in the obese population ($BMI \geq 30.0 \text{ kg/m}^2$), it increased further to 75.27% (Quek et al. 2023). We found that WSF decreased the body weight significantly of model mice from 7 weeks after administration compared to the MC group, and the weight gain of 17 weeks also decreased with significance. Additionally, liver and epididymis adipose mass weight declined significantly in the model mice, implying less lipid deposition in organs. Clinically, the disease progression of NAFLD is positively correlated with the serum levels of AST and ALT (Chinese Society of Endocrinology et al. 2018). It was identified that WSF had salient hepatoprotective effects due to reduced serum levels of AST and ALT in our study. Despite its inherent constraints, liver biopsy continues to be the gold standard for the course of NAFLD diagnosis and prognosis (Wang and Malhi 2018). H&E and Oil Red O staining results demonstrated that WSF could reverse pathological syndromes like steatosis, ballooning degeneration and inflammatory cell aggregation of hepatocytes caused by the HSHF diet. Meanwhile, NAS score reduction further proved the protective effects of WSF on hepatocyte lesions.

In 2020, an international panel advocated rechristening NAFLD as metabolic associated fatty liver disease (MAFLD) in an effort to underscore the metabolic underpinnings of the NAFLD pathogenesis course (Eslam et al. 2020). Our results showed that WSF could improve lipid metabolism by significantly modulating the serum and liver levels of TG and HDL-c, but it had no obvious effects on TC and LDL-c. Researches have indicated that excessive intake of bile salts not only causes an increase in intestinal absorption of cholesterol but also reduces the excretion of cholesterol by inhibiting the conversion to bile acids, leading to excessive accumulation of

cholesterol in the plasma and liver of the organism (Song et al. 2015; Xiao et al. 2023; Tilg et al. 2022). LDL is the primary carrier of cholesterol in plasma, transporting cholesterol from the liver to peripheral tissues, and accumulation of cholesterol-enriched LDL is a hallmark of hypercholesterolemia (Islam et al. 2022). Moreover, clinical research data have also demonstrated that high hepatic and plasma cholesterol accompanied high levels of LDL-c with were seen in obeticholic acid administration patients (Neuschwander-Tetri et al. 2015). Our experimental observations revealed that neither the positive drug nor the WSF manifested substantial reductions in serum or liver TC levels and serum LDL-c levels. This lack of significant reduction implies that the cholesterol and sodium cholate-supplemented diet has elicited an extremely severe perturbation in the organism's cholesterol metabolism. In conclusion, these results denoted that WSF could exert its anti-NAFLD efficacy mainly by ameliorating lipid metabolism partially and recovering liver inflammation and steatosis injury.

Furthermore, WSF exhibits a significant dose-dependent regulatory effect on glucose and lipid metabolism in rats with metabolic disorders, akin to the manifestations observed in NAFLD mice. However, the precise dose-dependent relationship of WSF in NAFLD models remains to be definitively established, due to variations in experimental animal strains and dietary compositions. Concurrently, WSF does not demonstrate significant toxic effects in normal mice at a dosage 12 times that of the human clinical dose. The observed significant differences in body weight may be attributed to the relatively higher initial body weight of the WS mice or potentially due to WSF enhancing their metabolic efficiency. The underlying mechanism warrants further investigation, particularly focusing on the activities of enzymes involved in glycolipid metabolism.

Network pharmacology has emerged as a potent strategy for holistically discerning the therapeutic targets of drugs in relation to diseases, owing to its capability of synthesizing colossal datasets to conduct virtual screenings grounded in both TCM ingredients and correlated symptoms (Zhong et al. 2023; Zhang et al. 2023). In the study combined with HPLC-Q-TOF/MS and network pharmacology, we attained 72 active components and 254 intersection target proteins. Sequentially, we further obtained NAFLD-related hub genes including TNF, IL6, AKT1, IL1B, PPARG and PTGS2, which played important roles in NAFLD abnormal metabolic pathways, corresponding to the degree values of the PPI interaction network. We have noticed that TNF- α , IL-6, IL-1 β and PTGS2 (COX2) are all inflammatory factors, as well as inflammation is also supposed to be an important driver of NAFLD and the progression to NASH (Rohm et al. 2022; Luo and Lin 2021). Thus, we further gauged the gene counts and confidence levels of inflammation related pathways. The KEGG analysis showed that all the gene counts of TNF, IL-17, Toll-like receptor and NF- κ B signaling pathway were all greater than 15 with *P* values less than 0.01, indicating the key role of these pathways of WSF on NAFLD treatment. Therefore, inflammatory related TLR4 and NF- κ B were also considered as the pivotal target proteins of WSF to alleviate NAFLD.

The outcomes from molecular docking analyses revealed that crucial components in WSF demonstrated high binding activities with pivotal targets comprised in inflammation related pathways (including TLR4, NF- κ B, COX-2, IL-1 β , IL-6 and TNF- α), with all minimum binding energies recorded at less than -5.0 kcal/mol (Tong et al. 2021; Zhou et al. 2022). This further confirmed the critical role of inflammatory pathways acquired from network pharmacology, particularly the TLR4/NF- κ B/COX-2 pathway, in the molecular mechanism of WSF on NAFLD treatment. Furthermore, we found that the majority of active components with both lower binding energies to proteins and higher degree values in the network belonged to the saponins of *Gynostemmae Herba*. Our prior researches have similarly demonstrated that gypenosides could ameliorate hepatic inflammation in high-fat diet induced NAFLD rats by attenuating the LPS/TLR4/MyD88/NF- κ B signaling pathway (Shen et al. 2020, 2022). Moreover, gypenosides could modulate associated enzyme functions involved in cholesterol production, fatty acid synthesis, transportation and degradation to improve lipid disorder in NAFLD as well (Zhou et al. 2023; Cheng et al. 2024). Those above implied that gypenosides could be the core bioactive ingredients of WSF, which need in-depth study later. In conclusion, WSF might exert pharmacological effects against NAFLD

by mediating activities of inflammatory related proteins of TLR4/NF- κ B/COX-2 pathway, which would be verified in the subsequent experiments.

The hepatic inflammation response is a crucial feature of NAFLD, and the canonical TLR4/NF- κ B inflammatory pathway has been identified as a critical contributor in the advancement of NAFLD (Tang et al. 2023). In normative hepatocytic contexts devoid of stimulatory cues, NF- κ B complexes with its cytoplasmic inactivator, the inhibitor of NF- κ B (I κ B), to form a suppressive ensemble that curtails the transcriptional activation potential of NF- κ B (Wei et al. 2022). Upon stimulation of hepatocytes, TLR4 engages with the downstream adaptor protein of myeloid differentiation factor 88 (MyD88) and initiates a signaling cascade that subsequently activates the I κ B kinase (IKK). This activation further prompts the phosphorylation and degradation of the I κ B protein, leading to a dissociation of the NF- κ B/I κ B protein complex, which is crucial for the transcriptional regulation of inflammatory responses (Feng et al. 2020). Moreover, NF- κ B activation leads to the production of pro-inflammatory cytokines comprising IL-1 β , IL-6 and TNF- α , which are prominently implicated in the progression of NAFLD (Liu et al. 2019; Lv et al. 2023).

Experimental evidence has illustrated the impairment of linoleic and arachidonic acid metabolism in the liver of NAFLD mice induced by the high fat diet with a significant upregulation of hepatic TLR4 expression, leading to a substantial accumulation of inflammatory cytokines (Qin et al. 2023). Linoleic acid is categorized as an n-6 polyunsaturated fatty acids, whose downstream metabolite is arachidonic acid in vivo, and holds a significant role in mediating inflammatory processes (Burns et al. 2018). COX-2 is a formidable enzyme that facilitates the conversion of arachidonic acid into prostaglandins and instigates inflammation subsequent to activation by a myriad of inflammatory stimuli encompassing cytokines and bacteria (Hu et al. 2020). It has been manifested that excessive linoleic acid intake could result in liver steatosis, inflammation injury and fibrotic response with higher levels of hepatic TG and free fatty acids (FFAs) (Graham et al. 2023). Moreover, it would also promote NF- κ B translocation and COX-2 activation, and induce production of proinflammatory cytokines like IL-1 β , IL-6 and TNF- α by the release of arachidonic acid derived compounds (Marchix et al. 2015).

Our results revealed a marked decrease in the expression levels of TLR4, NF- κ B and COX-2 in the liver tissue by WSF intervention compared with the NAFLD mice. As integrators of the inflammatory pathway in NAFLD, inactivation of NF- κ B and COX-2 could lead to less secretion of pro-inflammatory cytokines like IL-1 β , IL-6 and TNF- α (Huang et al. 2019; Cheng et al. 2013), which

was consistent with the ELISA results in this study. Combined with the previous results of HPLC-Q-TOF/MS, bioinformatics and molecular docking, we supposed that WSF treatment could ameliorate hepatic lipid disorder and inflammation injury in NAFLD through regulation of the TLR4/NF- κ B/COX-2 signaling pathway.

Conclusions

This study indicated that WSF could be used to alleviate NAFLD caused by the HSHF diet via improving fat accumulation, lipid metabolism, liver function and pathological damage. Moreover, a new insight was provided into the mechanisms through the TLR4/NF- κ B/COX-2 pathway combined with HPLC-Q-TOF/MS, bioinformatics, molecular docking and validation results. In addition, these results offer a pharmacological foundation for further product development and clinical implementation of WSF.

Abbreviations

ALT	Alanine aminotransferase
ASPL	Average shortest path length
AST	Aspartate transaminase
BNC	Betweenness centrality
BP	Biological process
CC	Cellular component
CNC	Closeness centrality
COX-2	Cyclooxygenase 2
DL	Drug-like properties
EA	Epididymis adipose
GLU	Glucose
GO	Gene ontology
HDL-c	High density lipoprotein cholesterol
HSHF	High-sucrose and high-fat
IHC	Immunohistochemistry
IL-1 β	Interleukin-1 β
IL-6	Interleukin-6
KEGG	Kyoto encyclopedia of genes and genomes
LDL-c	Low density lipoprotein cholesterol
MF	Molecular function
NAFLD	Nonalcoholic fatty liver disease
NAS	NAFLD activity score
NF- κ B	Nuclear factor- κ B
OB	Oral bioavailability
PPI	Protein-protein interaction
RT	Retention time
TC	Total cholesterol
TCM	Traditional Chinese medicine
TG	Triglyceride
TIC	Total ion chromatogram
TLR4	Toll-like receptor 4
TNF- α	Tumor necrosis factor α
WB	Western blot
WSF	Wang's empirical formula

Supplementary Information

The online version contains supplementary material available at <https://doi.org/10.1186/s10020-024-01022-3>.

Additional file 1.

Additional file 2.

Acknowledgements

All the authors would like to thank the researchers and staff of the mentioned software and databases.

Author contributions

SH Chen: Writing – review & editing, Methodology and Supervision; CJ Zhou: Writing and Data Collation; JH Huang: Writing and Data Acquisition; YL Qiao: Visualization and Software; N Wang: Data Acquisition and Analysis; YZ Huang: Method Investigation and Validation; B Li: Writing – review & editing and Methodology; WF Xu: Methodology; XL He: Methodology; KG Wang: Supervision; YH Zhi: Project Management; GY Lv: Funding acquisition and Supervision; SH Shen: Funding acquisition, Supervision and Methodology.

Funding

This study was supported by the National Natural Science Foundation of China (Nos. 81503527 and 82274134), the National Key Research and Development Plan (Nos. 2017YFC1702200 and 2017YFC1702202), the Key Research and Development Program of Zhejiang Province (No. 2020C04020), and Science and Technology Department of the State Administration of Traditional Chinese Medicine-Zhejiang Province Joint Project (No. GZY-ZJ-KJ-24068).

Availability of data and materials

No datasets were generated or analysed during the current study.

Declarations

Ethics approval and consent to participate

The Animal Ethics Committee of the Zhejiang University of Technology ratified the experiment plan (No. 20211119097, 19–11-2021).

Consent for publication

Not applicable.

Competing interests

The authors declare no competing interests.

Author details

¹Collaborative Innovation Center of Yangtze River Delta Region Green Pharmaceuticals, Zhejiang University of Technology, No. 18, Chaowang Road, Gongshu District, Hangzhou 310014, Zhejiang, China. ²Disease Prevention and Health Management Center, The First Affiliated Hospital of Zhejiang Chinese Medical University, Hangzhou 310006, Zhejiang, China. ³Zhejiang Provincial Key Laboratory of TCM for Innovative R & D and Digital Intelligent Manufacturing of TCM Great Health Products. Huzhou, Zhejiang 313200, China. ⁴College of Pharmaceutical Science, Zhejiang Chinese Medical University, No. 548, Binwen Road, Binjiang District, Hangzhou 310053, Zhejiang, China. ⁵Kun-Gen Wang National Famous Chinese Medicine Doctor Studio, Hangzhou 310006, Zhejiang, China.

Received: 2 July 2024 Accepted: 1 December 2024

Published online: 27 December 2024

References

- Anderson EL, Howe LD, Jones HE, Higgins JP, Lawlor DA, Fraser A. The prevalence of non-alcoholic fatty liver disease in children and adolescents: a systematic review and meta-analysis. *PLoS ONE*. 2015;10(10): e0140908.
- Bai LJ, Wu C, Lei SH, Zou M, Wang SJ, Zhang ZY, et al. Potential anti-gout properties of Wuwei Shexiang pills based on network pharmacology and pharmacological verification. *J Ethnopharmacol*. 2023;305: 116147.
- Berardo C, Di Pasqua LG, Cagna M, Richelmi P, Vairetti M, Ferrigno A. Nonalcoholic fatty liver disease and non-alcoholic steatohepatitis: current issues and future perspectives in preclinical and clinical research. *Int J Mol Sci*. 2020;21(24):9646.
- Bessone F, Razori MV, Roma MG. Molecular pathways of nonalcoholic fatty liver disease development and progression. *Cell Mol Life Sci*. 2019;76(1):99–128.

- Burns JL, Nakamura MT, Ma DWL. Differentiating the biological effects of linoleic acid from arachidonic acid in health and disease. *Prostaglandins Leukot Essent Fatty Acids*. 2018;135:1–4.
- Buzzetti E, Pinzani M, Tsochatzis EA. The multiple-hit pathogenesis of non-alcoholic fatty liver disease (NAFLD). *Metabolism*. 2016;65(8):1038–48.
- Chalasanani N, Younossi Z, Lavine JE, Charlton M, Cusi K, Rinella M, et al. The diagnosis and management of nonalcoholic fatty liver disease: practice guidance from the American association for the study of liver diseases. *Hepatology*. 2018;67(1):328–57.
- Chen J, Liu J, Wang Y, Hu XM, Zhou F, Hu YM, et al. Wogonin mitigates nonalcoholic fatty liver disease via enhancing PPAR α /AdipoR2, in vivo and in vitro. *Biomed Pharmacother*. 2017;91:621–31.
- Chen M, Xie Y, Gong S, Wang Y, Yu H, Zhou T, et al. Traditional Chinese medicine in the treatment of nonalcoholic steatohepatitis. *Pharmacol Res*. 2021a;172: 105849.
- Chen L, Ji X, Wang M, Liao X, Liang C, Tang J, et al. Involvement of TLR4 signaling regulated-COX2/PGE2 axis in liver fibrosis induced by *Schistosoma japonicum* infection. *Parasit Vectors*. 2021b;14(1):279.
- Chen J, Yang S, Luo H, Fu X, Li W, Li B, et al. Polysaccharide of *Atractylodes macrocephala* Koidz alleviates NAFLD-induced hepatic inflammation in mice by modulating the TLR4/MyD88/NF- κ B pathway. *Int Immunopharmacol*. 2024;141: 113014.
- Cheng Q, Li N, Chen MQ, Zheng JM, Qian ZP, Wang XY, et al. Cyclooxygenase-2 promotes hepatocellular apoptosis by interacting with TNF- α and IL-6 in the pathogenesis of nonalcoholic steatohepatitis in rats. *Dig Dis Sci*. 2013;58(10):2895–902.
- Cheng BB, Lv GY, Wu HS, Zheng X, Huang JH, He XL, et al. Exploring the mechanism of action of hawthorn to improve metabolic hypertension based on network pharmacology and molecular docking. *Chin J Mod Appl Pharm*. 2023;40(24):3377–88.
- Cheng SC, Liou CJ, Wu YX, Yeh KW, Chen LC, Huang WC. Gypenoside XIII regulates lipid metabolism in HepG2 hepatocytes and ameliorates non-alcoholic steatohepatitis in mice. *Kaohsiung J Med Sci*. 2024;40(3):280–90.
- Chinese Society of Endocrinology, Chinese Medical Association. Consensus on the diagnosis and treatment of non-alcoholic fatty liver disease and related metabolic disorders. *J Clin Hepatol*. 2018;34(10):2103–8.
- Day CP, James OF. Steatohepatitis: a tale of two “hits”? *Gastroenterology*. 1998;114(4):842–5.
- Deng GH, Zhao CC, Cai X, Zhang XQ, Ma MZ, Lv JH, et al. Untargeted metabolomics and TLR4/NF- κ B signaling pathway analysis reveals potential mechanism of action of *Dendrobium huoshanense* polysaccharide in nonalcoholic fatty liver disease. *Front Pharmacol*. 2024;15:1374158.
- Dong YG, Guo YF, Hu DY, Li Y, Li JJ. Expert consensus on safety evaluation of statins. *Chin J Cardiol*. 2014;42(11):890–4.
- Eslam M, Newsome PN, Sarin SK, Anstee QM, Targher G, Romero-Gomez M, et al. A new definition for metabolic dysfunction-associated fatty liver disease: an international expert consensus statement. *J Hepatol*. 2020;73(1):202–9.
- Fan JG, Kim SU, Wong VW. New trends on obesity and NAFLD in Asia. *J Hepatol*. 2017;67(4):862–73.
- Fang TY, Wang H, Pan XY, Little PJ, Xu SW, Weng JP. Mouse models of nonalcoholic fatty liver disease (NAFLD): pathomechanisms and pharmacotherapies. *Int J Biol Sci*. 2022;18(15):5681–97.
- Feng ZW, Pang LJ, Chen SY, Pang XH, Huang YS, Qiao Q, et al. Didymin ameliorates dexamethasone-induced non-alcoholic fatty liver disease by inhibiting TLR4/NF- κ B and PI3K/Akt pathways in C57BL/6J mice. *Int Immunopharmacol*. 2020;88:10.
- Goyal NP, Schwimmer JB. The progression and natural history of pediatric nonalcoholic fatty liver disease. *Clin Liver Dis*. 2016;20(2):325–38.
- Graham DS, Liu G, Arasteh A, Yin XM, Yan S. Ability of high fat diet to induce liver pathology correlates with the level of linoleic acid and Vitamin E in the diet. *PLoS ONE*. 2023;18(6): e0286726.
- Han X, Zhao W, Zhou Q, Chen H, Yuan J, Xiaofu Z, et al. Procyanidins from hawthorn (*Crataegus pinnatifida*) alleviate lipid metabolism disorder via inhibiting insulin resistance and oxidative stress, normalizing the gut microbiota structure and intestinal barrier, and further suppressing hepatic inflammation and lipid accumulation. *Food Funct*. 2022;13(14):7901–17.
- Houttu V, Csader S, Nieuwdorp M, Holleboom AG, Schwab U. Dietary interventions in patients with non-alcoholic fatty liver disease: a systematic review and meta-analysis. *Front Nutr*. 2021;8: 716783.
- Hsu WF, Sheen LY, Lin HJ, Chang HH. A review of western and Traditional Chinese medical approaches to managing nonalcoholic fatty liver disease. *Evid Based Complement Alternat Med*. 2016;2016:6491420.
- Hu Y, Yang XF, Wu SD, Xiao JH. COX-2 in liver fibrosis. *Clin Chim Acta*. 2020;506:196–203.
- Huang L, Ding W, Wang MQ, Wang ZG, Chen HH, Chen W, et al. Tanshinone IIA ameliorates non-alcoholic fatty liver disease through targeting peroxisome proliferator-activated receptor gamma and toll-like receptor 4. *J Int Med Res*. 2019;47(10):5239–55.
- Islam MM, Hlushchenko I, Pfisterer SG. Low-density lipoprotein internalization, degradation and receptor recycling along membrane contact sites. *Front Cell Dev Biol*. 2022;10:826379.
- Jiang HY, Gao HY, Li J, Zhou TY, Wang ST, Yang JB, et al. Integrated spatially resolved metabolomics and network toxicology to investigate the hepatotoxicity mechanisms of component D of *Polygonum multiflorum* Thunb. *J Ethnopharmacol*. 2022;298: 115630.
- Jiao X, Jin X, Ma Y, Yang Y, Li J, Liang L, et al. A comprehensive application: molecular docking and network pharmacology for the prediction of bioactive constituents and elucidation of mechanisms of action in component-based Chinese medicine. *Comput Biol Chem*. 2021;90: 107402.
- Jin ZL, Han K, Chen HY, Zhang XY, Qiao WL, Jia BX. Exploration of phytochemicals and biological functions of *Kadsura coccinea* pericarpium based on LC-MS and network pharmacology analysis and experimental validation. *J Funct Foods*. 2023;103: 105493.
- Kaur T, Madgulkar A, Bhalekar M, Asgaonkar K. Molecular docking in formulation and development. *Curr Drug Discov Technol*. 2019;16(1):30–9.
- Kleiner DE, Brunt EM, Van Natta M, Behling C, Contos MJ, Cummings OW, et al. Design and validation of a histological scoring system for nonalcoholic fatty liver disease. *Hepatology*. 2005;41(6):1313–21.
- Lei SS, Li B, Chen YH, He XL, Wang YZ, Yu HH, et al. *Dendrobii Officinalis*, a traditional Chinese edible and officinal plant, accelerates liver recovery by regulating the gut-liver axis in NAFLD mice. *J Funct Foods*. 2019;61: 103458.
- Li J, Zou BY, Yeo YH, Feng YM, Xie XY, Lee DH, et al. Prevalence, incidence, and outcome of non-alcoholic fatty liver disease in Asia, 1999–2019: a systematic review and meta-analysis. *Lancet Gastroenterol Hepatol*. 2019a;4(5):389–98.
- Li B, Lei SS, Su J, Cai XM, Xu H, He X, et al. Alcohol induces more severe fatty liver disease by influencing cholesterol metabolism. *Evid Based Complement Alternat Med*. 2019b;2019:7095684.
- Li YJ, Li S, Xue XY, Wang T, Li XJ. Integrating systematic pharmacology-based strategy and experimental validation to explore mechanism of Tripterium glycoside on cholangiocyte-related liver injury. *Chin Herb Med*. 2022;14(4):563–75.
- Liu BB, Deng XL, Jiang QQ, Li GX, Zhang JL, Zhang N, et al. Scoparone alleviates inflammation, apoptosis and fibrosis of non-alcoholic steatohepatitis by suppressing the TLR4/NF- κ B signaling pathway in mice. *Int Immunopharmacol*. 2019;75: 105797.
- Liu LL, Xu LM, Wang SJ, Wang LL, Wang XN, Xu HF, et al. Confirmation of inhibiting TLR4/MyD88/NF- κ B signalling pathway by duhuo jisheng decoction on osteoarthritis: a network pharmacology approach-integrated experimental study. *Front Pharmacol*. 2022;12: 784822.
- Loomba R, Friedman SL, Shulman GI. Mechanisms and disease consequences of nonalcoholic fatty liver disease. *Cell*. 2021;184(10):2537–64.
- Lu Y, Feng TT, Zhao JX, Jiang PF, Xu DX, Zhou ML, et al. Polyene phosphatidylcholine ameliorates high fat diet-induced non-alcoholic fatty liver disease via remodeling metabolism and inflammation. *Front Physiol*. 2022;13:810143.
- Luo YF, Lin H. Inflammation initiates a vicious cycle between obesity and non-alcoholic fatty liver disease. *Immun Inflamm Dis*. 2021;9(1):59–73.
- Lv SQ, Zhang ZY, Su XH, Li WD, Wang XY, Pan BC, et al. Qingrequzhuo capsule alleviated methionine and choline deficient diet-induced nonalcoholic steatohepatitis in mice through regulating gut microbiota, enhancing gut tight junction and inhibiting the activation of TLR4/NF- κ B signaling pathway. *Front Endocrinol*. 2023;13:1106875.
- Ma J, Fox CS, Jacques PF, Speliotes EK, Hoffmann U, Smith CE, et al. Sugar-sweetened beverage, diet soda, and fatty liver disease in the Framingham Heart Study cohorts. *J Hepatol*. 2015;63(2):462–9.
- Marchix J, Choque B, Kouba M, Fautrel A, Catheline D, Legrand P. Excessive dietary linoleic acid induces proinflammatory markers in rats. *J Nutr Biochem*. 2015;26(12):1434–41.

- Molavi F, Namazi N, Asadi M, Sanjari M, Motlagh ME, Shafiee G, et al. Comparison common equations for LDL-C calculation with direct assay and developing a novel formula in Iranian children and adolescents: the CASPIAN V study. *Lipids Health Dis.* 2020;19(1):129.
- Neuschwander-Tetri BA, Loomba R, Sanyal AJ, Lavine JE, Van Natta ML, Abdelmalek MF, et al. Farnesoid X nuclear receptor ligand obeticholic acid for non-cirrhotic, non-alcoholic steatohepatitis (FLINT): a multicentre, randomised, placebo-controlled trial. *Lancet.* 2015;385(9972):956–65.
- Porras D, Nistal E, Martínez-Flórez S, Pisonero-Vaquero S, Olcoz JL, Jover R, et al. Protective effect of quercetin on high-fat diet-induced non-alcoholic fatty liver disease in mice is mediated by modulating intestinal microbiota imbalance and related gut-liver axis activation. *Free Radic Biol Med.* 2017;102:188–202.
- Qin Y, Fan RY, Liu YX, Qiu SY, Wang L. Exploring the potential mechanism of *Rubus corchorifolius* L. fruit polyphenol-rich extract in mitigating non-alcoholic fatty liver disease by integration of metabolomics and transcriptomics profiling. *Food Funct.* 2023;14(20):9295–308.
- Quek J, Chan KE, Wong ZY, Tan C, Tan B, Lim WH, et al. Global prevalence of non-alcoholic fatty liver disease and non-alcoholic steatohepatitis in the overweight and obese population: a systematic review and meta-analysis. *Lancet Gastroenterol Hepatol.* 2023;8(1):20–30.
- Ren SM, Zhang QZ, Jiang M, Chen ML, Xu XJ, Wang DM, et al. Systematic characterization of the metabolites of defatted walnut powder extract in vivo and screening of the mechanisms against NAFLD by UPLC-Q-exactive orbitrap MS combined with network pharmacology. *J Ethnopharmacol.* 2022;285: 114870.
- Rohm TV, Meier DT, Olefsky JM, Donath MY. Inflammation in obesity, diabetes, and related disorders. *Immunity.* 2022;55(1):31–55.
- Romero-Gómez M, Zelber-Sagi S, Trenell M. Treatment of NAFLD with diet, physical activity and exercise. *J Hepatol.* 2017;67(4):829–46.
- Rosqvist F, Iggman D, Kullberg J, Cedernaes J, Johansson HE, Larsson A, et al. Overfeeding polyunsaturated and saturated fat causes distinct effects on liver and visceral fat accumulation in humans. *Diabetes.* 2014;63(7):2356–68.
- Shen SH, Jiang ZX, Sun J, Wang KG. An analysis of Professor Wang Kungen's experience in the diagnosis and treatment of metabolic syndrome. *J Zhejiang Chin Med Univ.* 2018;42(6):415–8.
- Shen SH, Wang KG, Zhi YH, Shen W, Huang LQ. Gypenosides improves nonalcoholic fatty liver disease induced by high-fat diet induced through regulating LPS/TLR4 signaling pathway. *Cell Cycle.* 2020;19(22):3042–53.
- Shen SH, Wang KG, Zhi YH, Dong Y. Gypenosides counteract hepatic steatosis and intestinal barrier injury in rats with metabolic associated fatty liver disease by modulating the adenosine monophosphate activated protein kinase and Toll-like receptor 4/nuclear factor kappa B pathways. *Pharm Biol.* 2022;60(1):1949–59.
- Shi TT, Wu L, Ma WJ, Ju LP, Bai MH, Chen XW, et al. Nonalcoholic fatty liver disease: pathogenesis and treatment in traditional Chinese medicine and western medicine. *Evid Based Complement Alternat Med.* 2020;2020:8749564.
- Shi WB, Wang ZX, Liu HB, Jia YJ, Wang YP, Xu X, et al. Study on the mechanism of Fufang E'jiao Jiang on precancerous lesions of gastric cancer based on network pharmacology and metabolomics. *J Ethnopharmacol.* 2023;304: 116030.
- Song P, Rockwell CE, Cui JY, Klaassen CD. Individual bile acids have differential effects on bile acid signaling in mice. *Toxicol Appl Pharmacol.* 2015;283(1):57–64.
- Sun YL, Tan ZF, Jiang ZY, Li M, Wang WQ, Huang YY, et al. Comparative efficacy and safety of traditional Chinese patent medicine for NAFLD in childhood or adolescence: a protocol for a Bayesian network meta analysis. *Medicine (Baltimore).* 2021;100(3): e24277.
- Tang YL, Zhu L, Tao Y, Lu W, Cheng H. Role of targeting TLR4 signaling axis in liver-related diseases. *Pathol Res Pract.* 2023;244: 154410.
- Tilg H, Adolph TE, Trauner M. Gut-liver axis: Pathophysiological concepts and clinical implications. *Cell Metab.* 2022;34(11):1700–18.
- Tilg H, Byrne CD, Targher G. NASH drug treatment development: challenges and lessons. *Lancet Gastroenterol Hepatol.* 2023;8(10):943–54.
- Tong HJ, Yu MT, Fei CH, Ji D, Dong JJ, Su LL, et al. Bioactive constituents and the molecular mechanism of *Curcuma Rhizoma* in the treatment of primary dysmenorrhea based on network pharmacology and molecular docking. *Phytomedicine.* 2021;86: 153558.
- Trott O, Olson AJ. Software news and update autodock vina: improving the speed and accuracy of docking with a new scoring function, efficient optimization, and multithreading. *J Comput Chem.* 2010;31(2):455–61.
- Wang XJ, Malhi H. Nonalcoholic fatty liver disease. *Ann Intern Med.* 2018;169(9):itc65–itc80.
- Wang LY, Du ZY, Guan Y, Wang B, Pei YL, Zhang LZ, et al. Identifying absorbable bioactive constituents of Yupingfeng powder acting on COVID-19 through integration of UPLC-Q/TOF-MS and network pharmacology analysis. *Chin Herb Med.* 2022;14(2):283–93.
- Wei PH, Jiang YP, Deng CY. The essence of "When one sees a disease of the liver, one knows that the liver transmits to the spleen, so one should first strengthen the spleen." *Lishizhen Med Mater Med Res.* 2015;26(11):2732–3.
- Wei W, Liu LM, Liu XK, Tao Y, Gong JY, Wang Y, et al. Black ginseng protects against Western diet-induced nonalcoholic steatohepatitis by modulating the TLR4/NF- κ B signaling pathway in mice. *J Food Biochem.* 2022;46(12): e14432.
- Wu PX, Liang SF, He YP, Lv R, Yang BD, Wang M, et al. Network pharmacology analysis to explore mechanism of Three Flower Tea against non-alcoholic fatty liver disease with experimental support using high-fat diet-induced rats. *Chin Herb Med.* 2022;14(2):273–82.
- Wu X, Zhang Y, Zheng D, Yin Y, Peng M, Wang J, et al. Prediction of the mechanisms of action of Qutan Huoxue decoction in non-alcoholic steatohepatitis (NASH): a network pharmacology study and experimental validation. *Pharm Biol.* 2023;61(1):520–30.
- Xiao J, Dong L-W, Liu S, Meng F-H, Xie C, Lu X-Y, et al. Bile acids-mediated intracellular cholesterol transport promotes intestinal cholesterol absorption and NPC1L1 recycling. *Nat Commun.* 2023;14(1):6469.
- Xiong YZ, Peng QW, Cao CM, Xu ZJ, Zhang B. Effect of different exercise methods on non-alcoholic fatty liver disease: a meta-analysis and meta-regression. *Int J Environ Res Public Health.* 2021;18(6):3242.
- Yagami T, Koma H, Yamamoto Y. Pathophysiological roles of cyclooxygenases and prostaglandins in the central nervous system. *Mol Neurobiol.* 2016;53(7):4754–71.
- Yang H, Xuefeng Y, Shandong W, Jianhua X. COX-2 in liver fibrosis. *Clin Chim Acta.* 2020;506:196–203.
- Younossi Z, Anstee QM, Marietti M, Hardy T, Henry L, Eslam M, et al. Global burden of NAFLD and NASH: trends, predictions, risk factors and prevention. *Nat Rev Gastroenterol Hepatol.* 2018;15(1):11–20.
- Younossi Z, Tacke F, Arrese M, Sharma BC, Mostafa I, Bugianesi E, et al. Global perspectives on nonalcoholic fatty liver disease and nonalcoholic steatohepatitis. *Hepatology.* 2019;69(6):2672–82.
- Zhang SS, Li JX. Consensus opinion of experts in traditional Chinese medicine: diagnosis and treatment of nonalcoholic fatty liver disease (2017). *J Tradit Chin Med.* 2017;58(19):1706–10.
- Zhang SS, Li QG, Li JX. Consensus opinion on chinese medicine diagnosis and treatment of non-alcoholic fatty liver disease (2009, Shenzhen). *Chin J Integr Tradit West Med Dig.* 2010;18(4):276–9.
- Zhang HY, Ge SN, Diao FY, Song W, Zhang Y, Zhuang PW, et al. Network pharmacology integrated with experimental verification reveals the antipyretic characteristics and mechanism of Zi Xue powder. *Pharm Biol.* 2023;61(1):1512–24.
- Zheng S, Xue C, Li S, Zao X, Li X, Liu Q, et al. Chinese medicine in the treatment of non-alcoholic fatty liver disease based on network pharmacology: a review. *Front Pharmacol.* 2024;15:1381712.
- Zhi GG, Shao BJ, Zheng TY, Mu J, Li JW, Feng YY, et al. Exploring the molecular mechanism of Gan Shuang granules for the treatment of non-alcoholic steatohepatitis using network pharmacology, molecular docking, and experimental verification. *Front Pharmacol.* 2023;14:1082451.
- Zhong YH, Liang J, Qin Q, Wang YJ, Peng YM, Zhang T, et al. The activities and mechanisms of intestinal microbiota metabolites of TCM herbal ingredients could be illustrated by a strategy integrating spectrum-effects, network pharmacology, metabolomics and molecular docking analysis: Platycodin D as an example. *Phytomedicine.* 2023;115: 154831.
- Zhou F, Zhou JH, Wang WX, Zhang XJ, Ji YX, Zhang P, et al. Unexpected rapid increase in the burden of NAFLD in China from 2008 to 2018: a systematic review and meta-analysis. *Hepatology.* 2019;70(4):1119–33.

- Zhou WJ, Zhu ZY, Xiao XL, Li CL, Zhang L, Dang YQ, et al. Jiangzhi granule attenuates non-alcoholic steatohepatitis by suppressing TNF/NFκB signaling pathway-a study based on network pharmacology. *Biomed Pharmacother.* 2021;143: 112181.
- Zhou BC, Qian ZH, Li QY, Gao Y, Li MH. Assessment of pulmonary infectious disease treatment with Mongolian medicine formulae based on data mining, network pharmacology and molecular docking. *Chin Herb Med.* 2022;14(3):432–48.
- Zhou TT, Cao LG, Du YM, Qin L, Lu YL, Zhang QR, et al. Gypenosides ameliorate high-fat diet-induced nonalcoholic fatty liver disease in mice by regulating lipid metabolism. *PeerJ.* 2023;11: e15225.

Publisher's Note

Springer Nature remains neutral with regard to jurisdictional claims in published maps and institutional affiliations.